

APPLICATION OF THE RHENIUM-OSMIUM ISOTOPE GEOCHRONOMETER TO  
NEOPROTEROZOIC AND PALEOZOIC ORGANIC RICH MUDROCKS

---

A Thesis

Presented to

the Faculty of the Department  
of Earth and Atmospheric Sciences

University of Houston

---

In Partial Fulfillment

of the Requirements for the Degree of

Master of Science

---

By

Steven A. Braun

December, 2012

## **Acknowledgements:**

Without the friendship and mentoring of two fantastic professors, Dr. Guilherme Gualda and Dr. Brendan Bream, I would never have ended up in graduate school. To them I owe the very existence of this work. Next, I would like to thank Dr. Alan Brandon. Without his dedicated guidance, I might never have been able to achieve all that I have in my time at University of Houston. I knew he would make a fantastic advisor when I came to visit during spring break of 2010. Of course the only people in the department that day were the geochemists Al and Dr. Tom Lapen. To Dr. Lapen, I owe another debt of gratitude. Despite his myriad commitments, he was always supportive and interested in the progress of my research. I owe a great many thanks to Dr. Francis Macdonald and his entire research team. Without their support and organization, I would never have been able to visit the Coal Creek Inlier, Yukon. Dr. Bill Dupre was a wonderful help to me early in my graduate career. His course Terrigenous Depositional Systems enabled me to bridge the gap between isotopic research and sedimentology. Dr. Eugene Domack has been a great outside collaborator. His willingness to share limited borehole material from Tasmania enabled new directions for this thesis. I owe a special debt of gratitude to Dr. David VanAcken and Dr. Robert Creaser. They opened their laboratory to me and without their eager collaboration this thesis would not be possible. I would also like to thank Shawn Wright and all the other graduate students at the UH for their friendship and collaboration. Lastly, I would like to give special thanks to my parents and sister.

APPLICATION OF THE RHENIUM-OSMIUM ISOTOPE GEOCHRONOMETER TO  
NEOPROTEROZOIC AND PALEOZOIC ORGANIC RICH MUDROCKS

---

An Abstract of a Thesis

Presented to

the Faculty of the Department  
of Earth and Atmospheric Sciences

University of Houston

---

In Partial Fulfillment

of the Requirements for the Degree of

Master of Science

---

By

Steven A. Braun

December, 2012

**Abstract:**

New Re-Os isotope data on organic-rich mudrocks (ORMs) from the Neoproterozoic Upper Fifteenmile Group, Coal Creek Inlier, Yukon Territory, Canada and the Paleozoic Quamby Fm., Turnbridge Borehole, Tasmania yield depositional model ages, which help to deconvolve the timing of complex tectonic and climatic changes in earth history. The Neoproterozoic Upper Fifteenmile Group has Re-Os depositional model age of  $764 \pm 51$  Ma ( $2\sigma$ ; Model-1; MSWD 4.2;  $O_s$   $0.37 \pm 0.19$ ). The age obtained is identical to ages from the same horizon across northwestern Canada. This result provides direct age control for biomineralizing microfossils and the Bitter Springs isotopic stage. If these model ages are correct, the Bitter Springs isotopic stage may be related to the Kiagas age glacial events in Africa and South America. The Paleozoic Quamby Fm. has a Re-Os model age of  $294 \pm 29$  Ma ( $2\sigma$ ; Model-3; MSWD 4.2;  $O_s$   $0.58 \pm 0.14$ ). This result is the first radiometric age obtained for the Quamby Fm. and is in good agreement with biostratigraphic control that suggests an Asselian age. This result also suggests that the end of the Late Paleozoic Ice Age in Tasmania is synchronous with other glacial deposits across Australia. In addition to discussing the implications of these Re-Os results, this thesis discusses the development of the Re-Os analytical method at the University of Houston.

**Table of Contents:**

<b><u>Chapter 1: Introduction to Re-Os Geochronology, Methods,</u></b>	<b>1</b>
<b><u>and Analytical Challenges</u></b>	
<b>Introduction to Re-Os Geochronology</b>	<b>1</b>
<i>History of Rhenium Osmium Geochronology</i>	1
<i>The Re-Os Chronometer in Organic-rich mudrocks (ORM)</i>	3
<i>The <sup>187</sup>Os/<sup>188</sup>Os Ratio: Tracing Global Climate Change</i>	8
<b>Rhenium and Osmium Extraction and Analytical Methods</b>	<b>9</b>
<i>Sample Collection</i>	9
<i>Sample Processing</i>	12
<i>Sample Digestion</i>	12
<i>Osmium Extraction Chemistry</i>	13
<i>Rhenium Extraction Chemistry</i>	15
<i>Analytical Procedures</i>	16
<b>Challenges in <sup>187</sup>Re-<sup>187</sup>Os Isotope Analytical Development</b>	<b>20</b>
<i>Rhenium Blanks from Ni Wire Filament</i>	20
<i>Blanks from Chromic Acid</i>	22
<b><u>Chapter 2: Re-Os Geochronology of the Upper Fifteenmile Group, Coal Creek Inlier,</u></b>	<b>26</b>
<b><u>Yukon Territory, Canada</u></b>	

<b>Introduction</b>	26
<b>Methods</b>	32
<b>Results</b>	35
<b>Discussion</b>	39
<i>Differences between Laboratories</i>	39
<i>Heterogeneity in <math>Os_i</math> in Samples from the Fifteenmile Group</i>	41
<i>Significance of the Re-Os Depositional Age of the Fifteenmile Group</i>	45
<b>Conclusions</b>	51
<b><u>Chapter 3: Preliminary Re-Os Geochronology of the Quamby Mudstone, Turnbridge</u></b>	<b>54</b>
<b><u>Borehole, Tasmania</u></b>	
<b>Introduction</b>	53
<b>Methods</b>	54
<b>Preliminary Results and Discussion</b>	55
<b><u>References</u></b>	58

## **Table of Figures:**

Figure 1: Schematic diagram of Re and Os chemical extraction procedures	10
Figure 2: Isochron of Exshaw Fm. from Creaser et al. (2002)	18
Figure 3: Results of Ni filament blank tests	21
Figure 4: Results of nitrogen bubbling cleaning experiment	25
Figure 5: Location of Coal Creek Inlier	27
Figure 6: Stratigraphy of the Coal Creek Inlier	33
Figure 7: Field photos showing sampling difficulties in the Fifteenmile Group	34
Figure 8: Preferred Re-Os depositional Model-1 age of the Upper Reefal Assemblage	37
Figure 9: Inter-laboratory comparison of total Re-Os measured and $^{187}\text{Re}/^{188}\text{Os}$ and $^{187}\text{Os}/^{188}\text{Os}$ ratios.	40
Figure 10: Weathering discrimination diagram	43
Figure 11: Correlation of Cryogenian age deposits across Alaska and Canada	47
Figure 12: Generalized stratigraphy of the Parmeener Supergroup, Tasmania	54
Figure 13: Preferred Isochron for the Quamby Mudstone, Turnbridge Borehole, Tasmania	57

## **Chapter 1: Introduction to Re-Os Geochronology, Methods, and Analytical Challenges**

### **Introduction to Re-Os Geochronology:**

#### *History of Rhenium Osmium Geochronology:*

Geochemists have utilized the  $^{187}\text{Re}$ - $^{187}\text{Os}$  isotope system as a chronometer for half a century (e.g. Clayton, 1964), dating a wide range of processes from the formation of the solar system (Luck et al., 1980) to differentiation of interiors of planets (e.g. Brandon et al., 2000). Yet for much of that time, one of the fundamental controls on the accuracy and precision of the isotope system, the half-life and decay constant of  $^{187}\text{Re}$ , was poorly constrained and remained controversial (Lindner et al, 1989; Smoliar et al, 1996; Shen et al, 1998; Shirey and Walker, 1998). The first determinations of the half-life had large uncertainties and were limited by the analytical techniques of the time (Naldrett and Libby, 1948; Herr et al., 1954; Hirt et al., 1963). Lindner and coworkers (1989) determined the accepted value for the half-life of  $^{187}\text{Re}$  to be  $4.23 \pm 0.13 \times 10^{10} \text{y}^{-1}$ . Smoliar et al. (1996) determined the decay constant of  $^{187}\text{Re}$   $\lambda = 1.666 \pm 0.0017 \times 10^{-11} \text{y}^{-1}$  which results in a half-life of  $^{187}\text{Re}$  of  $4.23 \pm 0.13 \times 10^{10} \text{y}^{-1}$ . This determination is identical to a calculation of the decay constant based on paired analyses of Re-Os and U-Pb isotope systems on a suite of ore bodies (Selby et al., 2007). The linkage of the two isotopic systems increases the robustness of the chronometer and enables the isotope system to be used on a wide range of materials ranging from iron meteorites, metal ores, peridotites, to volcanic lavas, that formed from the earliest

solar system times to those formed in the past few millions of years, providing that there was adequate initial fractionation of Re/Os ratio and closed system processes (Kendall, 2004; Dickin, 2008).

The earliest work on the  $^{187}\text{Re}$ - $^{187}\text{Os}$  isotope system was hampered by extremely high ionization potential of both Re and Os ( $\sim 9\text{eV}$ , Dickin, 2008). This ruled out analysis of these metals by positive ion Thermal Ionization Mass Spectrometry TIMS. A number of alternative methods were developed to work around the ionization efficiency problem with varying degrees of success. Among the methods developed were Resonance Ionization Mass Spectrometry (RIMS; Walker and Fassett, 1986), Inductively Coupled Plasma Mass Spectrometry (ICPMS; Russ et al., 1987), and Secondary Ionization Mass Spectrometry (SIMS; Allègre and Luck, 1980). The development of Negative Thermal Ionization Mass Spectrometry (N-TIMS; Creaser et al., 1991; Volkening et al., 1991) dramatically improved the ionization efficiency of Re and Os enabling much more precise measurements. Modern analytical techniques can yield accurate and precise Re and Os isotope measurements to better than  $\pm 0.5\%$   $2\sigma$  (Selby and Creaser, 2003) at very low concentrations (nanogram and subnanogram respectively; Rooney et al., 2011). The precision now obtainable makes the study of Re and Os well suited for a wide variety of earth materials, including Organic-rich Mudstones (ORM).

*The Re-Os Chronometer in Organic-rich Mudrocks (ORM):*

One recently developed application of the  $^{187}\text{Re}$ - $^{187}\text{Os}$  isotope chronometer is the dating of ORM. The application of the  $^{187}\text{Re}$ - $^{187}\text{Os}$  isotope chronometer to organic rich sediments adds the ability to correlate stratigraphic sections utilizing absolute timing. This technique offers the important ability to ground truth potentially more problematic relative dating methods like paleobiology, petrographic facies associations, or chemostratigraphy. This is especially true for the Neoproterozoic sections where the relative paucity of suitable rock types such as volcanoclastic units limit application of isotopic systems like U-Pb or Rb-Sr (eg. Halverson, 2005; Halverson et al, 2010). In the case of Neoproterozoic sedimentary sequences,  $^{187}\text{Re}$ - $^{187}\text{Os}$  isotope chronometry of ORM can thus be important in providing absolute age constraints for sections where relative age control is ascribed by litho-, bio-, and stable isotope stratigraphy.

Both Re and Os present in the world's oceans are derived from three main sources: continental runoff, hydrothermal venting, and extraterrestrial debris (Pheucker Ehrinbrink and Ravizza, 2000). Rhenium and Os accumulate in sediments through two main mechanisms, reductive capture into sediments and adsorption onto organic molecules. Rhenium occurs as the  $\text{ReO}_4^-$  species in seawater (Anbar et al., 1992 and Colodner et al., 1993). Experimental data indicates that in oxic conditions  $\text{ReO}_4^-$  ions preferentially stay in solution and tend not to bind with minerals or organic material (Yamashita et al., 2007). Both empirical data from organic-rich sediments in reducing environments and experimental data from organic rich sediments deposited under

anoxic conditions show enrichment in Re suggesting reductive capture from seawater (Ravizza et al., 1991; Crusius et al., 1996; Cohen et al., 1999; Selby and Creaser, 2003; Yamashita et al., 2007; Morford et al., 2012). Emerging evidence questions the suggestion of pure reductive capture of Re and suggests that Re coprecipitation with a Fe-Mo-S phase is required to enrich Re in sediments (Helz and Dolor, 2012). However, the precise removal relationship between Re, sediments, and organic material remains unclear and is an important avenue for future research. Osmium functions slightly different than Re and can leave seawater during oxic conditions, concentrating in ferromagnesian minerals (Yamashita et al., 2007). Although under reducing conditions there is experimental and empirical evidence of reductive capture of Os into sediments (Koide et al., 1991; Ravizza et al., 1991; Cohen et al., 1999; Woodhouse et al., 1999; Levasseur et al., 2000; Selby and Creaser, 2003; Yamashita et al., 2007). In reductive systems, Yamashita et al. (2007) find that Os concentrates in multiple phases of sediment, particularly organic matter and Fe-Mg oxides. However, like Re, the precise mechanisms controlling where Os resides in organic matter are unclear and require further research.

Further understanding of Re and Os removal from seawater is required to confirm the three fundamental principles of  $^{187}\text{Re}$ - $^{187}\text{Os}$  isotope chronometry are met. The three principles are: 1) the Re and Os in ORMs are hydrogenous in origin; 2) the ORMs being dated have a homogenous  $\text{Os}_i$ , reflecting the seawater reservoir at the time of deposition; and 3) the ORMs analyzed are a closed system with respect to Re

and Os since the time of deposition (Kendall et al., 2004, 2009). The findings of Yamashita et al. (2007) have significant importance for the  $^{187}\text{Re}$ - $^{187}\text{Os}$  isotope chronometer because they present evidence of the complex associations of Re and Os in sediments and suggest that care must be taken to ensure that only hydrogenous Re and Os are measured. The following section documents the development of the chronometer and highlights important works that add confidence that the fundamental assumptions of  $^{187}\text{Re}$ - $^{187}\text{Os}$  isotope chronometry are met.

The seminal work of Ravizza and Turekian (1989) demonstrated the ability of the  $^{187}\text{Re}$ - $^{187}\text{Os}$  isotope chronometer to accurately constrain the age of the well-studied Mississippian/Devonian boundary in the Bakken Shale. They conclude based on good correlations between paleobiology in the Bakken and the model age yielded by  $^{187}\text{Re}$ - $^{187}\text{Os}$  isotope chronometry that the system is relatively difficult to disturb after deposition and lithification. However, modern sediments from the Black Sea show that Os concentrations and  $^{187}\text{Os}/^{188}\text{Os}$  ratios of bulk ORMs show significant mixing between organic material and continental detritus, causing scatter in Os isotopic initial ratios and therefore decreasing the accuracy and precision of a  $^{187}\text{Re}$ - $^{187}\text{Os}$  isochron (Ravizza et al, 1991). To prevent detrital contamination, accurate age measurements must be made from analyses that specifically access the organic component of ORM, which is assumed to draw their Re and Os from a uniform homogeneous source (seawater).

The subsequent decade of Re-Os research on ORM refined the robustness of the chronometer. Work on Jurassic shales in England confirmed that the  $^{187}\text{Re}$ - $^{187}\text{Os}$  isotope

system closes shortly after deposition and accurately retains the Os isotopic signal of seawater (Cohen et al, 1999). Work in the Exshaw Fm. showed that for immature through overmature ORM (Tmax 421–485 °C), once closed, the  $^{187}\text{Re}$ - $^{187}\text{Os}$  isotope system remains undisturbed through the oil window (Creaser et al., 2002). However, both works noted geologic scatter related to a detrital Os component. As earlier work found, this reduced the precision and accuracy of  $^{187}\text{Re}$ - $^{187}\text{Os}$  isochrons on ORM. It would take the development of a new analytical method to reduce detrital Os contamination further. In 2003, Selby and Creaser reported a new  $\text{CrO}_3$ - $\text{H}_2\text{SO}_4$  digestion method, replacing the aqua regia method, which reduced isochron errors by roughly an order of magnitude. Most of the error reduction is attributed to leaving behind the detrital Re and Os component, and the geologic scatter associated with it, by selectively accessing the organic component of Re and Os in ORM. Subsequent work has confirmed that the  $\text{CrO}_3$ - $\text{H}_2\text{SO}_4$  digestion method yields more accurate and precise  $^{187}\text{Re}$ - $^{187}\text{Os}$  isotope model ages (eg. Kendal et al, 2004, Rooney et al., 2011). The  $\text{CrO}_3$ - $\text{H}_2\text{SO}_4$  digestion method is now considered standard practice for obtaining the hydrogenous  $^{187}\text{Re}$ - $^{187}\text{Os}$  isotope systematics in ORM.

With two decades of foundation work on Re and Os in ORM, much recent work in the field has dealt with sorting out complications to and improving accuracy of the  $^{187}\text{Re}$ - $^{187}\text{Os}$  isotope chronometer. Modeling work based on ORM data from the Atar group, West Africa by Rooney et al. (2010) suggests that  $^{187}\text{Re}$ - $^{187}\text{Os}$  isotope age determinations can be significantly more resilient to contact metamorphism than other

isotope systems, such as Rb-Sr, and remain undisturbed to temperatures up to ~650°C. Due to this resiliency, multiple works now report the  $^{187}\text{Re}$ - $^{187}\text{Os}$  isotope chronometer being a useful oil source fingerprinting tool, especially in non-traditional and biodegraded reservoirs (Selby and Creaser, 2005; Selby et al., 2007; Finley et al., 2011; Finley et al., 2012). However, as multiple works report, not all  $^{187}\text{Re}$ - $^{187}\text{Os}$  isotope ORM data sets are immune from resetting or alteration. These works commonly associate these problems with hydrothermal fluid circulation and either the loss, gain, or both of Re and Os (Kendal et al., 2009; Yang et al., 2009). Despite yielding accurate and precise results when the chronometer works, concerns remain about the viability of collecting  $^{187}\text{Re}$ - $^{187}\text{Os}$  isotope data sets, which are both capital and time intensive.

Increasingly, research suggests that specific attention must be given to both the lithology and the sampling method to ensure the best sample suites are selected for  $^{187}\text{Re}$ - $^{187}\text{Os}$  isotope chronometry. Work by Baioumy et al. (2011) shows that depositional environment has an important role on the sequestration of Re and Os from the seawater reservoir. Despite using an antiquated Ni-S fire assay measurement technique, their results suggest that only ORM deposited in fully marine settings accurately track the Re and Os budgets of seawater. The study finds that ORM deposited in terrestrial and marginal marine settings do not reflect the seawater reservoir budget of Re and Os. However, a study on the Eocene Green River Formation finds that lacustrine source rocks can yield accurate and precise  $^{187}\text{Re}$ - $^{187}\text{Os}$  isotope model ages (Selby, 2011), which

suggests that much important work remains to be done with respect to Re and Os partitioning into shales.

Once suitable ORM lithologies are identified effort must be taken to select the most suitable samples. Georgiev et al. (2012) confirm what many laboratories have suspected for some time, that core samples are comparatively much better candidates for  $^{187}\text{Re}$ - $^{187}\text{Os}$  isotope dating methods than outcrop samples. In some cases, weathered outcrop samples simply fail to yield a coherent isochron at all (Peucker-Ehrenbrink and Hannigan, 2000; Jaffe et al., 2002). In these cases it is suspected that oxygen, either from meteoric water or the atmosphere, has oxidized the organic matter causing chemical weathering of Os and particularly of Re. Despite these potential drawbacks many works, including this one, successfully obtain high precision isochrons from outcrop samples.

*The  $^{187}\text{Os}/^{188}\text{Os}$  Ratio: Tracing Global Climate Change:*

In addition to being a high-precision chronometer, the  $^{187}\text{Re}$ - $^{187}\text{Os}$  isotope system is also an excellent tracer of continental erosion and mid-ocean ridge magmatic activity (Sharma et al., 1999 and Singh et al., 1999). Osmium trapped in organic marine sediments record the  $^{187}\text{Os}/^{188}\text{Os}$  ratio in oceans at the time of deposition. Osmium has a residence time of 5-35 thousand years (Pegram et al., 2002 and Oxburg et al., 2007). On these timescales, the  $^{187}\text{Os}/^{188}\text{Os}$  ratio is considered homogeneously mixed throughout the world's oceans (Burton et al., 2010). These time scales enable the

$^{187}\text{Os}/^{188}\text{Os}$  ratio to track relatively short-term climatic fluctuations like glacial and interglacial periods (Peucker-Ehrenbrink and Ravizza, 2000). Because a principal source of radiogenic  $^{187}\text{Os}$  is continental detritus, positive fluctuations in the marine  $^{187}\text{Os}/^{188}\text{Os}$  record can provide valuable proxy evidence of changes in both physical and chemical weathering (Dalia and Ravizza, 2010). The primary controls on changes in weathering are glacial cover and orogeny (Dalia and Ravizza, 2010). Change in global magmatic activity at spreading centers and large igneous provinces are tracked by negative excursions in the marine  $^{187}\text{Os}/^{188}\text{Os}$  record, such as those recorded in Jurassic marine shales on the Atlantic margin (Cohen et al., 1999) and in black shales at Cenomanian-Turonian boundary (Turgeon and Creaser, 2008). Hence, the Os isotopic record of ORM can track the changes flux due to the combination of tectonic orogeny and glaciations, which control continental erosion rates.

### **Rhenium and Osmium Extraction and Analytical Methods:**

The following sections outline the steps taken to extract and measure Re and Os from ORMs. Figure 1 describes a schematic workflow of the Re and Os extraction process.

#### *Sample Collection:*

Collection of ORM samples for Re and Os measurement requires diligence as there are a number processes that affect Re and Os systematics in ORM, most notably weathering and  $\text{Os}_i$  heterogeneity. The negative impacts from these issues can be

## Re-Os Extraction Procedures

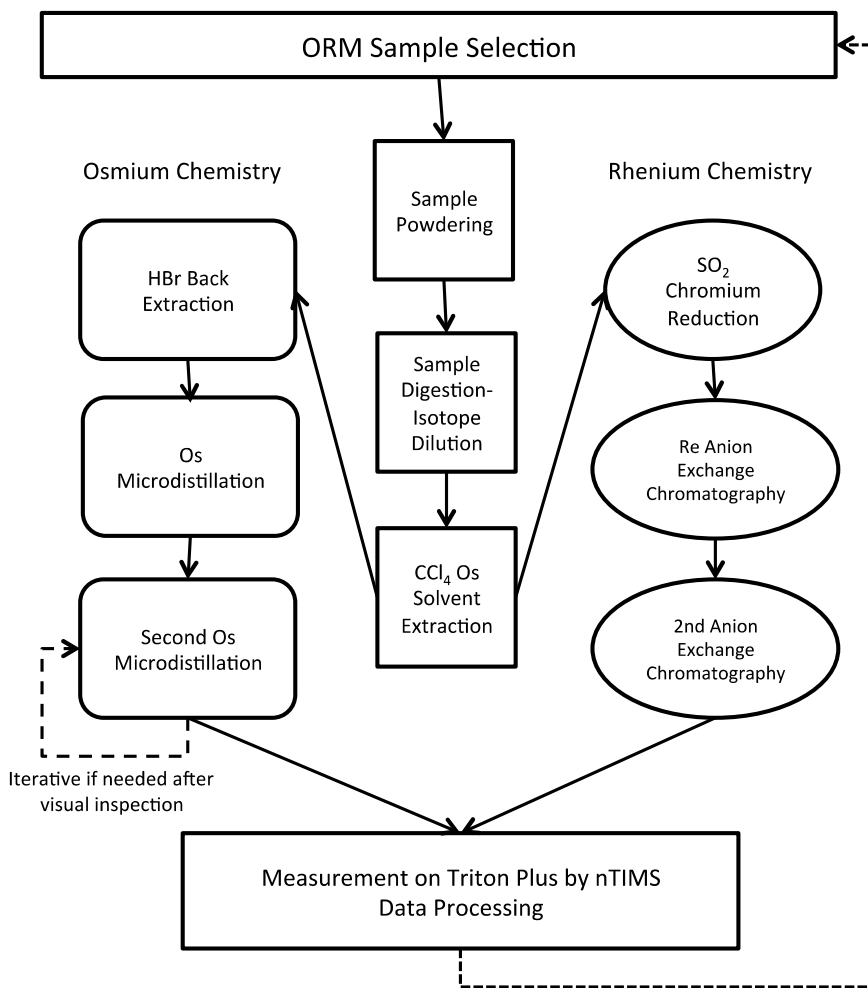


Figure 1: Schematic diagram of Re and Os chemical extraction procedures. Squares indicate extraction procedures performed for both Re and Os extraction. Rounded rectangles represent Os extraction procedures performed separately from Re extraction procedures. Ovals represent Re extraction procedures performed separately from Os extraction procedures.

minimized by proper sampling procedures. In order to minimize the effects of

weathering, every effort is made to select fresh outcrop samples. A fresh outcrop

sample will be devoid of soil material, fractures, rust staining, calcite veins, and other signs of post-depositional alteration. Taking steps to ensure samples selected meet these criteria help to minimize or eliminate post-depositional  $^{187}\text{Re}$ - $^{187}\text{Os}$  isotope disturbance. Obtaining truly fresh samples may be difficult from any outcrop sample. Work by Pierson-Wickmann et al. (2002) shows intense Re and Os weathering profiles up to 5m into an outcrop. Georgeiv et al. (2012) confirms these results and suggest that oxidation of organic material through weathering plays a substantial roll in the loss of Re and Os. Another way to introduce post-depositional disturbance is through sample collection in the presence of metal. Even minimal sample contact with metal can impact Re and Os abundances of ORM, which occur naturally on part per billion (ppb) and part per trillion (ppt) levels. All outcrop samples analyzed in this study were collected without metal contact and all core samples were polished using silicon carbide to remove all surfaces potentially affected by metal contact. Selecting the best sample suites for  $^{187}\text{Re}$ - $^{187}\text{Os}$  isotope analysis also requires obtaining an adequate spread in initial Re content without variations in the initial  $\text{Os}_i$ . Therefore the best sample suites will take at least 5 samples of a single ORM horizon horizontally across an outcrop while minimizing vertical displacement of the sample (<10cms). In core samples, this sampling procedure is not possible, so sample sets may sample vertically with the understanding that these data sets potentially introduce an amount of  $\text{Os}_i$  heterogeneity, and potentially decreasing the precision and accuracy of a reported isochron. The last factor that can influence sample selection is heterogeneity of Re-Os on a local scale. Rooney

(2011) suggests sample sizes between 100-300g are required to minimize sample heterogeneities. Samples collected for analysis in this study were typically about the size of a deck of cards and after removal of exposed surfaces typically yielded  $\geq 100$  grams.

*Sample Processing:*

Sample processing occurred in the rock crushing and clean labs of the University of Houston. Prior to crushing, all samples were visually inspected for surface oxidation and weathering. Samples with obvious weathering, fractures, and modern organic material (like lichen or moss) were set aside for later study. Sample suites selected for processing typically had at least 3 samples whose character was free from fractures and visual signs of weathering. The selected samples were cut with a tile saw to remove all exposed surfaces. The cut samples were polished to remove any cutting metal residue using coarse grit silicon carbide. At this point, samples were typically about the size of a domino, ~30-70 grams. Samples were crushed to small chips, ~0.5cm in the longest direction, using a ceramic mortar and pestle. The sample chips were powdered in a pre-cleaned ceramic shatterbox for 2 minutes. Typically, powdered samples yield between 15 and 50 grams of total material for carius tube digestion.

*Sample Digestion:*

All sample digestion procedures were performed in hepa-filtered, metal-free clean labs at the University of Houston and the University of Alberta under the direction of Professor Alan Brandon and Professor Robert Creaser, respectively. All sample Re and

Os determinations were made using a standardized isotope dilution process. Sample powders (0.3-1.0 grams) were weighed on a balance and loaded into a glass carius tube vessel. A dry ice and alcohol mixture was used to freeze the carius tube before loading a known amount of mixed  $^{185}\text{Re}$ - $^{190}\text{Os}$  spike. A rinse of 4ml 4N  $\text{H}_2\text{SO}_4$  was washed through the spike container and loaded into the carius tube to ensure maximum spike yield. After the sample, spike and the acid mixture had frozen, a 3-4ml aliquot of 0.5g/1ml  $\text{CrO}_3$ -4N  $\text{H}_2\text{SO}_4$  (chromic acid) solution was loaded and frozen. This solution preferentially accesses hydrogenous Re and Os and leaves the non-hydrogenous component in the residue (Selby and Creaser, 2003). This is important for obtaining precise  $^{187}\text{Re}$ - $^{187}\text{Os}$  isotope chronology because it minimizes potential mixing of the varied isotopic composition of the detrital component with the uniform seawater component (Ravizza and Turekian, 1989, Creaser et al., 2002, Selby and Creaser, 2003).

The carius tube was sealed while its contents remain frozen using a butane torch. The contents of the sealed carius tube were allowed to thaw before being vigorously shaken for ~5 minutes. The sealed carius tubes were loaded in to steel jackets and placed into an oven at ~240°C for 24-48 hours to ensure sample-spike equilibration. The digested sample -  $\text{CrO}_3$ -4N  $\text{H}_2\text{SO}_4$  was refrozen before being opened for Re and Os extraction chemistry.

#### *Osmium Extraction Chemistry:*

Sample osmium extraction uses solvent extraction, back extraction and

subsequent refinement through micro-distillation according to previously published methods (Cohen and Waters, 1996; Creaser et al., 2002, Selby and Creaser, 2003). Once opened, three 3ml rinses of carbon tetrachloride ( $\text{CCl}_4$ ) are added to the carius tubes prior to thawing. To minimize oxidative loss of Os, immediately upon thawing the  $\text{CCl}_4$  + digested sample mixture is placed into a pre-cleaned (dilute HCl) closed 50ml PFA centrifuge tube. The  $\text{CCl}_4$  acts as an organic solvent, readily extracting the  $\text{OsO}_4$  from the chromic acid mixture (Cohen and Waters, 1996). The sealed centrifuge tubes were shaken for 5 minutes to ensure maximum  $\text{OsO}_4$  extraction into the  $\text{CCl}_4$ . The mixture was centrifuged to separate the dense  $\text{CCl}_4$  +  $\text{OsO}_4$  phase from the less dense chromic acid mixture (which contains the Re). The dense  $\text{CCl}_4$  phase is pipetted into a glass vial containing 3ml of 9N (concentrated) HBr, sealed and heated to  $60^\circ\text{C}$  for 24 hours. This reaction back extracts (reduces) the  $\text{OsO}_4$  molecules to  $\text{OsBr}_6^-$ . The remaining chromic acid solution is set aside for Re chemistry.

After 24 hours the reduced  $\text{OsBr}_6^-$  - HBr solution was taken to near dryness (< $\sim 100\mu\text{l}$  remaining) on a pre-cleaned Teflon tape-coated watch glass. The remaining < $\sim 100\mu\text{l}$  of  $\text{OsBr}_6^-$  - HBr solution was taken to dryness on the cap of a pre-cleaned tri-star PFA microdistillation vial. The lid of the tri-star vial is loaded with  $\sim 20\mu\text{l}$  of 9N (concentrated) HBr. Slightly less than  $20\mu\text{l}$  of HBr can be used if the surface tension of the vial fails to hold the full  $20\mu\text{l}$  of HBr. About  $60\mu\text{l}$  of chromic acid solution was added to the dried down  $\text{OsBr}_6^-$  - HBr spot. The lid, containing the  $20\mu\text{l}$  of HBr, must be quickly fastened to the cap to prevent oxidative loss of volatile  $\text{OsO}_4$ . The sealed

microdistillation vial is placed on a hot plate not hotter than 80°C for about 12 hours. This process volatilizes the reduced Os from the dried sample spot into OsO<sub>4</sub> and then reduces the Os once again into HBr in the tip of the microdistillation vial. This step was performed twice unless visual inspection of the twice-distilled OsBr<sub>6</sub><sup>-</sup> salts show evidence of impurity, such as green coloration or excess cloudy white clumps. The microdistillation process can be performed up to 4 times before yield and blank addition issues result in the likely analysis being untrustworthy because of reduction in sample Os yield and/or increase in blank (Creaser, personal communication, 2012).

*Rhenium Extraction Chemistry:*

Rhenium extraction chemistry was slightly modified from Selby and Creaser (2003) and required reduction of the chromium acid solution followed by anion exchange chromatography. The remaining aliquot of chromic acid after osmium extraction was transferred to 15ml PFA 15ml centrifuge tubes. The 50ml centrifuge tubes were rinsed using MiliQ 18.2 ohm H<sub>2</sub>O. After rinsing, 6ml of MiliQ 18.2 ohm H<sub>2</sub>O and 3ml of the remaining chromic acid solution were added to the 50ml centrifuge tube. Utilizing pasteur pipette tips, SO<sub>2</sub> was bubbled through the solution, reducing the chromium (VI) to chromium (III) through the reaction  $3\text{SO}_2 + 2\text{H}_2\text{CrO}_4 + 3\text{H}_2\text{O} \rightleftharpoons \text{Cr}_2(\text{SO}_4)_3 + 5\text{H}_2\text{O}$ . This step is of vital importance because of chromium (VI)'s propensity to complicate anion exchange chromatography (Selby and Creaser, 2003). Once reduced the chromic acid + water solution was run through preconditioned disposable polyethylene columns loaded with ~1ml of anion resin. Prior to running the chromic acid mixture, the anion

columns were cleaned with 6ml 6N HNO<sub>3</sub> and conditioned with 4ml 0.2 N HCl. After elution, a series of acids were passed through the anion resin to remove excess contaminants: 4ml 1N HCl, 1ml 0.2N HNO<sub>3</sub>, and 1.5ml 6N HNO<sub>3</sub>. The sample Re cut was removed from the anion resin with a 5ml 6N HNO<sub>3</sub> wash into a pre-cleaned PTFE collection beaker. The collected Re cut was taken to dryness at 80°C and then brought up in ~2ml of 0.2N HNO<sub>3</sub>. This column process was repeated a second time to purify the final Re cut.

*Analytical Procedures:*

Purified Re salts were loaded onto baked Ni filaments using 1µl of concentrated HNO<sub>3</sub> and taken to dryness. Approximately, 0.5 µl of barium nitrate was added to the filament, serving as an electron donor to improve ionization efficiency. Purified Os salts are loaded onto baked Pt filaments using 2 µl of concentrated HBr. Less than 0.5ul of barium hydroxide was added to the filament, serving as an electron donor to improve ionization efficiency. The loaded Ni and Pt filaments were then ready for measurement using (n-TIMS) following a standard protocol laid out in Creaser et al. (1991) and Volkening et al. (1991). Measurements of Re and Os were made on a Triton Plus at the University of Houston and a Micromass Sector 54 at the University of Alberta. Isotopic measurements of Re were made using a static Faraday collection mode and isotopic measurements of Os were made using a secondary electron multiplier in peak-hopping mode.

Standards were run during every analytical session to monitor data reproducibility. An in-house Os standard of identical composition to the Johnson Matthey Os standard reported in Brandon et al. (1999) was analyzed and yielded a  $^{187}\text{Os}/^{188}\text{Os}$  ratio of  $0.11386 \pm 0.00021$  ( $n=4$ ;  $2\sigma$ ). This value is identical within error to the reported value (Brandon et al., 1999). An in-house Re standard with identical composition to that reported in Creaser et al. (2002) was analyzed and yielded a  $^{185}\text{Re}/^{187}\text{Re}$  ratio of  $0.5980 \pm 0.0018$  ( $n=4$ ;  $2\sigma$ ). This value is identical within error of published values in both Creaser et al. (2002) and Gramlich (1973).

Procedural blanks for all data reported in this thesis are between  $\sim 0.2$  and  $1.1\text{pg}$  for Os and between  $27$  and  $32\text{pg}$  for Re. The average Os blank concentration was  $0.9 \pm 0.66\text{pg}$  ( $2\sigma$ ;  $n=5$ ) with an  $^{187}\text{Os}/^{188}\text{Os}$  ratio of  $0.1639 \pm 0.093$  ( $2\sigma$ ;  $n=5$ ). The average Re blank was  $0.02915 \pm 0.00247\text{ng}$  ( $2\sigma$ ;  $n=5$ ). For error propagation purposes, all measured blanks were assigned a  $\pm 30\%$  error, which closely approximates the variability of both Os blank concentration and blank  $^{187}\text{Os}/^{188}\text{Os}$  ratios.

All  $^{187}\text{Re}$ - $^{187}\text{Os}$  isotope model ages are calculated using the isochron method.

Figure 2 explains the Re-Os isochron diagram presentation. All  $^{187}\text{Re}$ - $^{187}\text{Os}$  isotope analyses were regressed using the *Isoplot V 4.15* using the isochron model (Ludwig, 2008). All data regressed are assigned  $\pm 2\sigma$  errors based on the combined propagation of blank abundances, spike calibration, and reproducibility of standard analyses. The

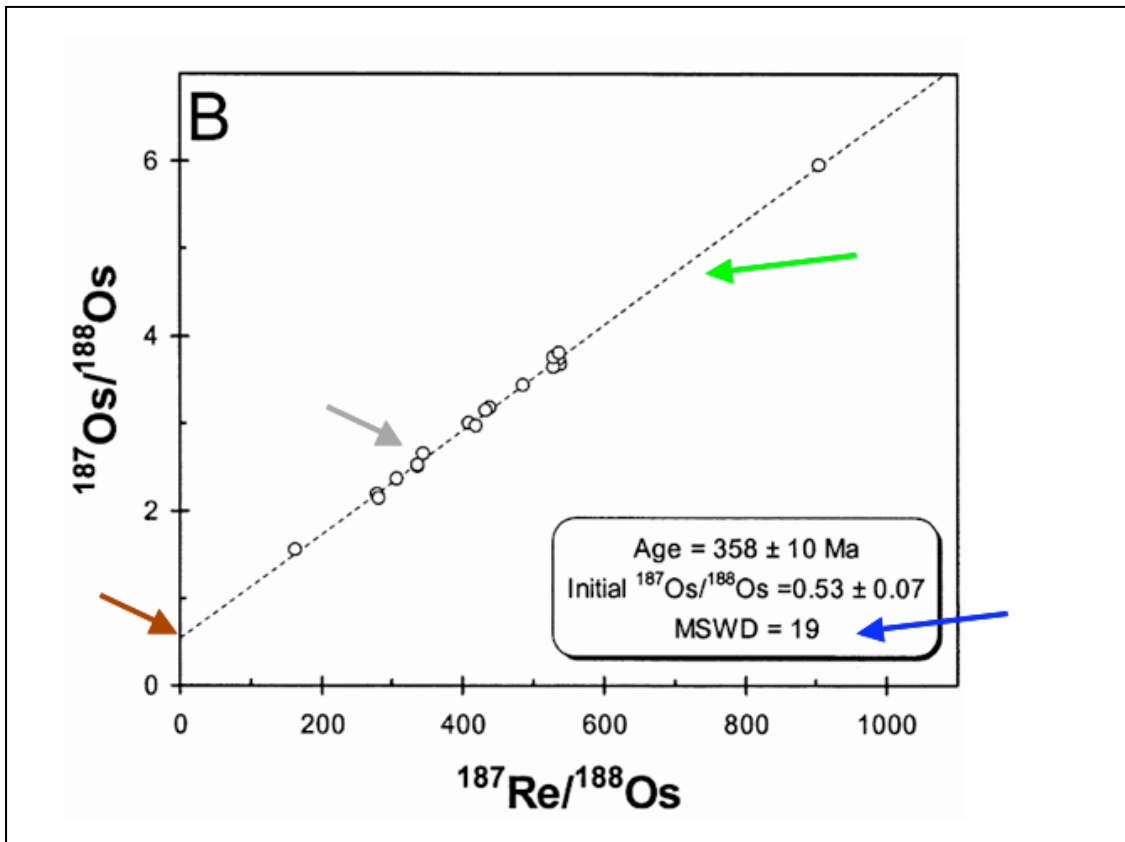


Figure 2: Isochron of Exshaw Fm. from Creaser et al (2002). Diagram modified to show important aspects of Isochron age presentation. Grey line indicates sample points. Green line indicates computed least squares regression line. Red line indicates calculated initial  $^{187}\text{Os}/^{188}\text{Os}$  ratio. Blue line indicates MSWD, interpreted to represent the amount of geologic scatter about the regression line.

propagation of these errors suggests that scatter about an isochron is not the result of analytical error. Additional assessment of errors was made using the error correlation

function ( $\rho$ ) and using multiple error assignments in *Isoplot*.  $\rho$  varies from -1 to 1. A  $\rho$  value of 1 represents a perfect positive correlation between the two axes, in the case of  $^{187}\text{Re}$ - $^{187}\text{Os}$  isochrons between  $^{187}\text{Re}/^{188}\text{Os}$  and  $^{187}\text{Os}/^{188}\text{Os}$ . A  $\rho$  value of zero represents no correlation between  $^{187}\text{Re}/^{188}\text{Os}$  and  $^{187}\text{Os}/^{188}\text{Os}$ . A low  $\rho$  value for data points is one method for determining if data points are altered and should be considered for exclusion. *Isoplot* can also address errors multiple ways by assigning different weights to errors as it calculates a model age from an isochron regression. A Model-1 solution assumes the analytical errors are the only reason data does not fit the isochron regression. A Model-2 solution calculates the isochron regression by assigning the regressed data equal weights by giving them zero-error correlations unlike a Model-1 solution. A Model-3 solution assumes that the scatter about the isochron is a combination of some unknown error (e.g. geologic scatter) and the analytical uncertainty (Ludwig, 2008; Rooney, 2011). All data presented here are either Model-1 or Model 3 solutions and when possible both solutions are presented to compare the results. Finally, to ensure that calculated isochrons are meaningful, the coherence of the isochron is measured by the mean square of weighted deviates (MSWD). The MSWD of a meaningful isochron should be less than ( $<5$ ). An MSWD of 1 would suggest that the errors of the data points about the isochron are entirely due to analytical uncertainty. MSWD's much lower than one can suggest that there is less scatter than expected or that analytical uncertainties may be overestimated. MSWDs much higher than 1 indicate that there is likely a source of geologic scatter about the isochron that cannot be

explained by analytical errors (Dickin, 2008).

### **Challenges in $^{187}\text{Re}$ - $^{187}\text{Os}$ Isotope Analytical Development:**

#### *Rhenium Blanks from Ni Wire Filament:*

One potential problem with Re measurements is Re blank from impure filaments. Despite using 99% pure metals basis Alfa Aesar Ni filament wire, filament blank tests determined unbaked Ni filament to contain measureable amounts of Re. In order to minimize this contamination, the filaments were glowed in air to oxidize any surficial Re on the filament wire. Figure 3 presents the results of a Ni-wire baking experiment. There are qualitative suggestions that filament batch F19 has lower blank abundances. However, further work would be required to conclusively determine if F19 is actually cleaner. Numerous other factors such as TIMS focus settings, loading procedure, and other user-defined parameters could result in the minor variations observed. In general, increasing the length of time the filaments were glowed decreased the measured amount of Re blank. The benefit of additional time glowed appears to disappear between 15 to 30 minutes. Laboratory observations have noted that heating Ni filaments longer than 30 minutes has the tendency weaken or break the Ni-filaments. To prevent the risk of losing a filament loaded with sample it would be prudent not to

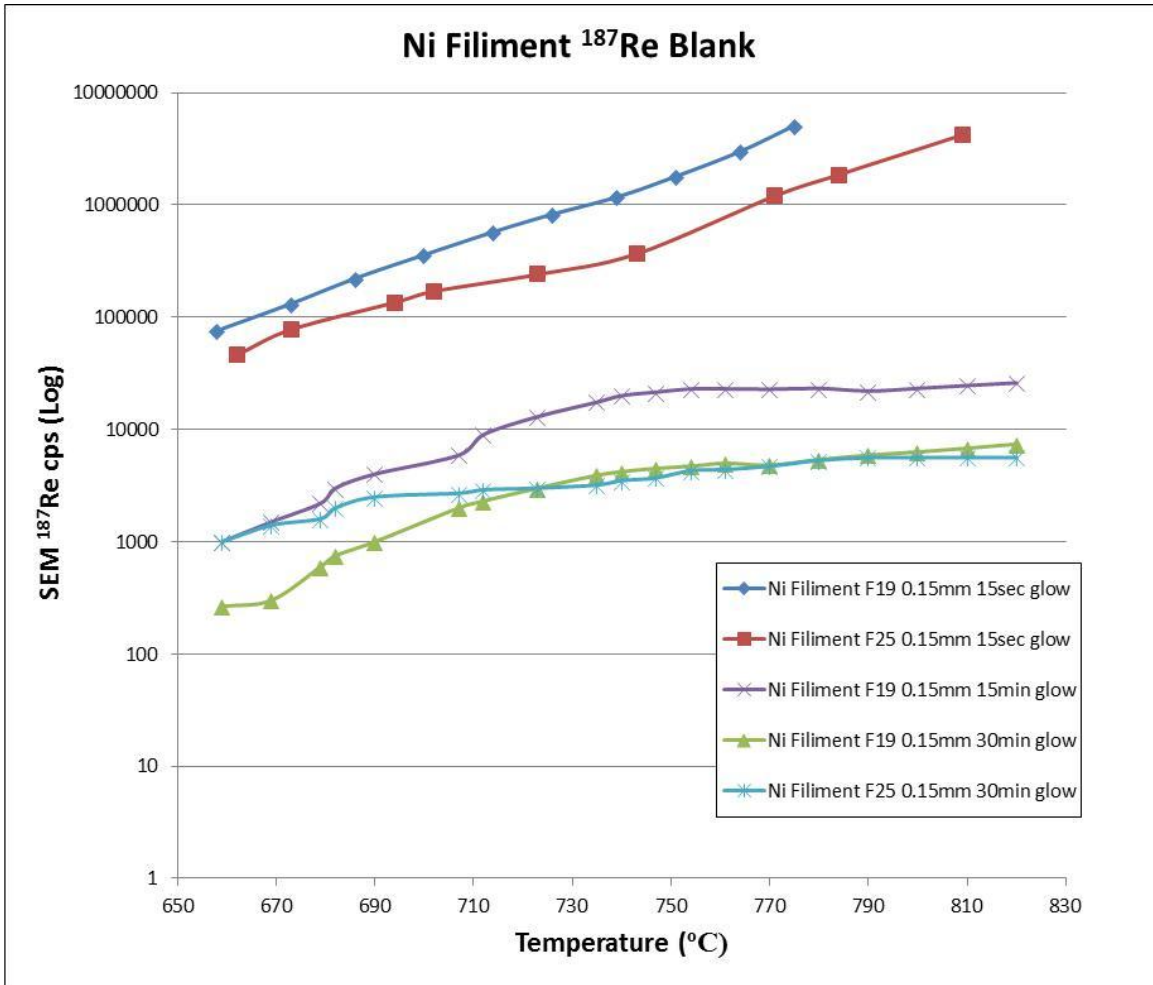


Figure 3: Results of Ni filament blank tests. Chart compares filament temperature with secondary electron multiplier counts per second. Note the decreasing amount of reduction on SEM counts between 15 and 30 minute glow times. Glow times over 30 minutes increase filament weakness and were not measured.

glow filaments much longer than 30 minutes. All measurements taken at the University of Houston were made using F19 filaments and were glowed for approximately 30 minutes. Assuming 160k counts is equivalent to ~1mV of current on a faraday collector, a conservative Re run intensity of 60mV, and normal Re run temperatures (750-800°C), filament blank will make up <0.2% of the total Re signal. This is a nominal amount and should not affect the accuracy and precision of Re analysis.

*Blanks from Chromic Acid:*

The CrO<sub>3</sub>-4N H<sub>2</sub>SO<sub>4</sub> solution is a major source of procedural blank. In particular, reagent Cr (VI) powder can contain high Os and Re abundances up to 100's of picograms per gram. High Re blank is a far larger issue than high Os blank and is not easily cleaned from chromic acid (Creaser Personal Communication, 2012). Obtaining Cr (VI) powder

<b>Chromic Acid Brand</b>	Avg. Re ppb	2σ	Avg. Os ppt	2σ	Avg. 187Os/188Os	2σ
<b>Sigma Aldrich</b>	46.1	15.1	0.724	0.432	0.173	0.110
<b>Puratronic</b>	30.7	0.6	0.865	0.923	0.171	0.0484
<b>Sigma Aldrich</b>	31.1	2.2	17.789	2.841	0.114	0.008
<b>Fluka</b>						

Table 1: Table shows average total procedural blanks for both Re and Os between chromic acids made with three different Cr(VI) powders. All Re-Os data presented in this thesis use chromic acid made from Puratronic Cr(VI) powder.

with the lowest Re blank is therefore the key control on the quality of the CrO<sub>3</sub>-4N H<sub>2</sub>SO<sub>4</sub> solution. However, problems arise when the chromic acid with the lowest Re blank has a high Os blank. This section discusses the results of blank tests on multiple chromic acid solutions as well as the results of attempts to clean the chromic acid solutions.

Table 1 shows the results of different total procedural blanks using chromic acids made from different brands of Cr (IV) oxide powder. The results suggest that there is significant variability between blanks made from different brands' powder as well as within the same batch of a single manufacturer of Cr VI oxide powder. Three brands of Cr (VI) oxide powder have been tested and total procedural blanks calculated for: Sigma Aldrich, Puratronic, and Sigma Aldrich Flucka. Sigma Aldrich total procedural blanks averaged  $0.724 \pm 0.432$  ppt ( $2\sigma$ ;  $n=4$ ) for Os and  $46.1 \pm 15.1$  ppb ( $1\sigma$ ; 4) for Re. Puratronic blanks averaged  $0.865 \pm 0.923$  ppt ( $2\sigma$ ;  $n=11$ ) for Os and  $30.7$  ppb  $\pm 0.6$  ( $1\sigma$ ;  $n=8$ ) for Re. Sigma Aldrich Fluka chromic acid blanks average  $17.78 \pm 2.8$  ppt ( $2\sigma$ ;  $n=5$ ) for Os and  $31.1 \pm 2.2$  ppb ( $2\sigma$ ;  $n=4$ ). Sigma Aldrich has acceptable Os blank levels but Re blank levels an order of magnitude higher than both Puratronic and SA Fluka chromic solutions. The high Re blank levels rule out Sigma Aldrich Cr (VI) oxide as a candidate for use in digestion of ORMs. Puratronic Cr (VI) oxide blank results have acceptable values for both Re and Os and is the chromic acid used for all data reported in this study. However, during the course of this thesis, the manufacturer discontinued the Puratronic product. Therefore, all future chromic acid digestions must be made with an alternative product. Sigma Aldrich Fluka Cr (VI) oxide is used by the University of Alberta and was recommended by Dr. Robert Creaser. The blank values using the Sigma Aldrich Fluka Cr (VI) oxide have acceptable Re blank values but poor Os blank values. The blanks gathered on the Sigma Aldrich Fluka chromic acid came from separate batches, which respectively had Os blanks of 21, 20.6, and 17.6 ppt. The batch with the lowest Os blank

was selected for use in Os cleaning experiments.

Once the  $\text{CrO}_3$ -4N  $\text{H}_2\text{SO}_4$  solution is prepared, one possible way to clean chromic acid of Os is to employ heat and heat and bubbled  $\text{GN}_2$ . To set up the cleaning procedure the  $\text{CrO}_3$ -4N  $\text{H}_2\text{SO}_4$  solution is attached to a custom designed coil condenser bubbler. The coil bubbler, connected to the  $\text{GN}_2$  source, flows gas through the solution and then escapes out the top into the fume hood. A heat tape is wrapped around the bottle containing the  $\text{CrO}_3$ -4N  $\text{H}_2\text{SO}_4$  solution, conducting a moderate heat ( $<80^\circ\text{C}$ ) through the mixture. The combination of the bubbled gas and heat could enable Os present in the mixture to volatilize out of the solution as gaseous  $\text{OsO}_4$ . The coil condenser preserves the original normality of the chromic acid solution. Because cold water is constantly pumped through the coil condenser, any evaporated water returns back to the sample. Figure 4 presents the results of the cleaning procedure. The cleaning procedure reduced total Os blanks only slightly ( $\sim 4$  ppt) over the course of a two-week cleaning period. Multiple explanations for this result include: contamination elsewhere in the procedure, human error, or the failure to effectively clean the Os from the chromic acid. The repeatedly high blank values suggest human error is not the cause of the high blanks. Contamination of the system or failure to clean the blanks could result in the results seen. One way to test this root cause is to attempt additional methods of cleaning the chromic acid solution. Further cleaning tests, including the use of solvent extraction, are ongoing and are outside the scope of this thesis.

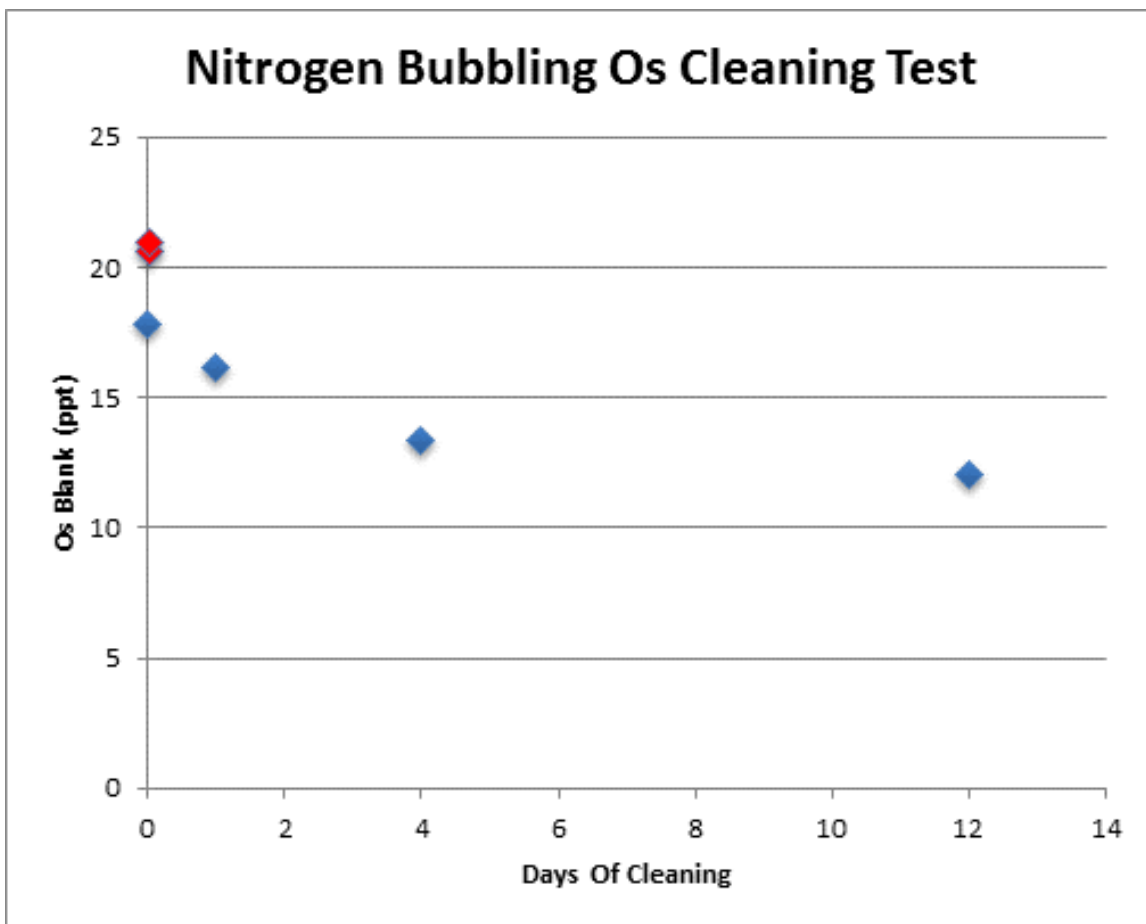


Figure 4: Results of nitrogen bubbling cleaning experiment on different batches of Sigma Aldrich Flucka chromic acid. Red diamonds are two different un-cleaned batches. The blue diamonds indicate progressive analyses of the lowest initial blank batch of Sigma Aldrich Flucka chromic acid.

## **Chapter 2: Re-Os Geochronology of the Upper Fifteenmile Group, Coal Creek Inlier, Yukon Territory, Canada**

### **Introduction:**

The Cryogenian period (~850-630Ma) of the Neoproterozoic records evidence of at least 2 widespread low-latitude glaciations (Schrag et al., 2002, Macdonald et al., 2010a, Evans and Raub, 2011), dramatic variations in seawater chemistry (eg Kaufman et al., 1997; Kasemann et al., 2005; Halverson et al., 2005; Canfield et al., 2007, 2008; Halverson and Shields-Zhou, 2011), and the diversification of complex life (e.g. Anbar et al., 2008). Exposures from the Cryogenian are found in three separate erosional inliers across ~1500 km from the border region of Alaska through the Northwest Territories (Macdonald and Roots, 2010). Figure 5 shows the field area and the regionally correlative Cryogenian sedimentary successions. Ongoing research suggests that these inliers are broadly correlative (Macdonald et al., 2010a; Macdonald et al., 2012 in press). Recent fieldwork examined a key sedimentary succession from the time period in the Coal Creek Inlier of the Yukon Territory, Canada.

The Coal Creek inlier in the Ogilvie Mountains offers an excellent field laboratory to study the interplay of between tectonics, climate, and life in the Cryogenian (~850-635Ma). The Cryogenian sequences in Coal Creek are purported to contain: (1) the Sturtian glacial interval, one of two purported snowball earth events in the Neoproterozoic (Macdonald et al., 2010a), (2) multiple the carbon isotope excursions

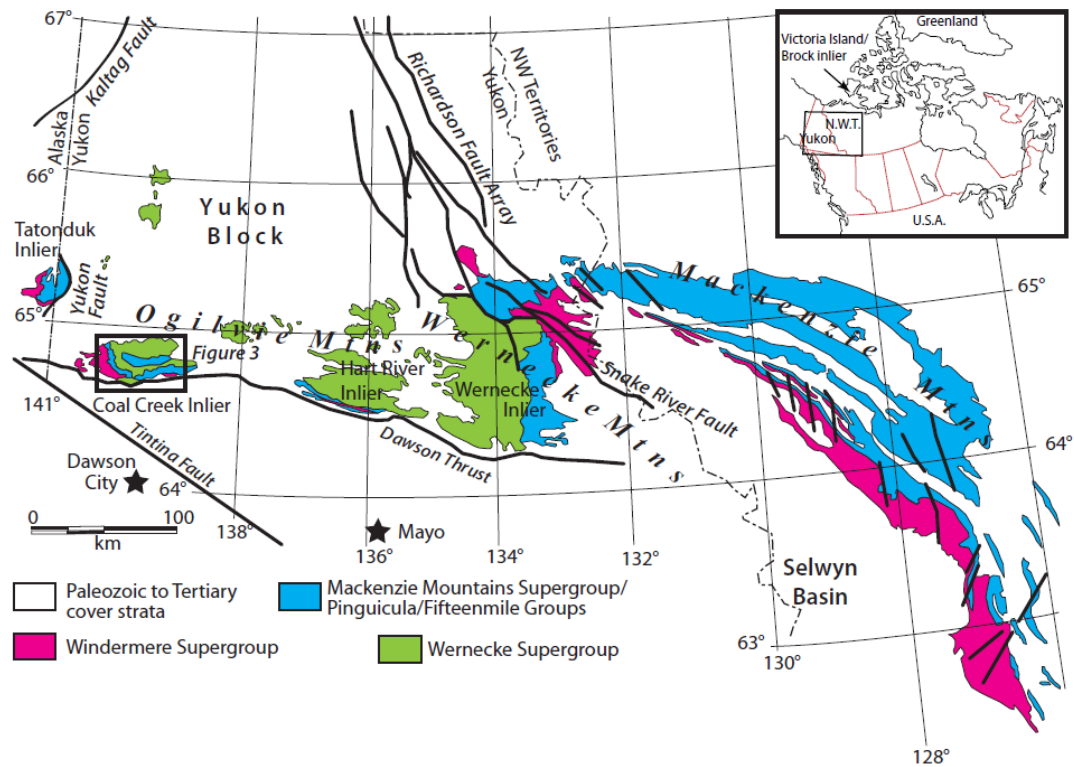


Figure 5: Location of Coal Creek Inlier. Figure from Macdonald et al. (2012, unpublished). Map shows three areas of age control for correlatives of the Upper Fifteenmile Group: Coal Creek inlier (U-Pb IDTIMS in zircon, Macdonald et al. 2010a; Re-Os, this work), the Tatonduk inlier (Zircon fission track; Bergman et al., 1993 unpublished), and the Victoria Islands (Re-Os, VanAcken et al., 2012)

~12‰  $\delta^{13}\text{C}_{\text{carb}}$ , both leading up to the Sturtian glacial event and during the ‘Bitter Springs’ isotope stage (Macdonald et al., 2010a; Macdonald et al., 2012, in press), (3) syn-depositional to early diagenetic talcs, possibly indicating unique Cryogenian sea water conditions as well as anaerobic respiration of microorganisms (Tosca et al., 2011), (4) banded iron formations (Hoffman and Halverson, 2011), and (5) early fossil evidence of biomineralization (Macdonald et al., 2010b and Cohen et al., 2011).

Evidence of glacially influenced and derived sediment is found in the Coal Creek inlier within the Rapitan Fm. (Macdonald and Roots, 2010), formerly PH1 (Thompson et al. 1987; Mustard and Roots, 1997). In the Coal Creek Inlier, the Rapitan Fm. can have thicknesses up to ~120m. The unit is recognized by its distinctive maroon basal limestones and is followed by >10m of interbedded brecciated tuff beds with massive diamictite. Sitting above the massive diamictite is a finely laminated carbonate mudstone which is penetrated by numerous dropstones. Some of these dropstones contain striated clasts, which are interpreted to be of glacial origin (Macdonald and Roots, 2010). Multiple glaciogenic structures are found within the Rapitan Fm. including plow structures and soft-sediment deformation. These structures may imply the sediments were deposited with proximity to grounded ice (Macdonald et al., 2010a)

In addition to the glacially derived sediments of the Rapitan Fm., multiple carbon isotope excursions are recorded in carbonates from measured sections throughout the Coal Creek Inlier. These isotope excursions are reported as  $\delta^{13}\text{C}_{\text{carb}}$  relative to the Vienna Pee Dee Belemnite Standard and are generally thought to reflect the carbon budget of the global ocean (Hosler, 1997). The isotope excursions noted in the Coal Creek Inlier are broadly correlative with similar isotopic excursions throughout the Canadian Cordillera (Halverson, 2006; Jones et al., 2010; Macdonald et al., 2010a) and globally in Australia and Svalbard (Hill et al., 2000; Halverson et al., 2005; Halverson and Shields-Zhou, 2011). The two carbon isotopic excursions record the Bitter Springs interval and the Sturtian glacial event. The Bitter Springs isotopic excursion may be

reflective of an unknown glacial event or a true polar wander event (Halverson et al., 2007). The carbon isotope excursion associated with the Sturtian glacial event is thought to reflect the general demise of photosynthetic life in the world's oceans due to ice cover (Macdonald et al., 2010a). However, these isotopic records can be problematic due to resetting, alteration, and even facies dependent control of isotopes (Frimmel, 2010). Recent evidence from the Coal Creek Inlier finds that some of the carbon isotope record can be varied spatially as well as temporally, suggesting that the importance of radiometric age control is critical for calibrating the Cryogenian carbon record (Macdonald et al., 2012 in press).

Beyond the dramatic temporal changes in ocean chemistry implied by the carbon isotope record, the deposition of sedimentary talc places constraints on the chemistry of Cryogenian ocean water. Experimental and field data suggest that the Cryogenian Ocean likely to produce depositional talc required a high pH, low detrital influx, high amounts of dissolved SiO<sub>2</sub>, increased Mg<sup>2+</sup>, and Fe respiring anaerobic bacteria (Tosca et al., 2011). These requirements lead to the recognition of the Cryogenian Ocean being unique from both the earlier Mesoproterozoic and the later Cambrian oceans (Tosca et al., 2011). Since <sup>187</sup>Os/<sup>188</sup>Os analysis has been used in other locations to suggest dynamic changes in earth's ocean chemistry (Cohen et al., 1999; Turgeon and Creaser, 2008), it may be possible to expand the knowledge of Neoproterozoic ocean chemistry through application of the <sup>187</sup>Os/<sup>188</sup>Os proxy.

In both the Coal Creek and the adjacent Tatonduk Inlier, the upper 10m of the Rapitan Fm. is composed of interbedded Fe-formations and finely laminated shale-siltstones with abundant dropstones (Macdonald and Cohen, 2011). Initially described by Young (1982), the Fe-formations have FeO concentrations up to ~50% and  $\text{SiO}_2/\text{Al}_2\text{O}_3$  ratios suggestive of chemical deposition with little clastic influence. Once attributed to rift-related hydrothermal activity (Young, 1988), the emerging view implies their relationship to terminal glacial sediments means that the Fe-formations were precipitated during the end of a long-lived glaciation (Macdonald and Cohen, 2011). A global glaciation could produce Fe-formations due to increased Fe solubility in a poorly oxygenated, ice covered ocean combined with a sudden oxygenation event at the end of a glacial period (Martin, 1965; Kirschvink, 1992). The reappearance of these beds within the Cryogenian after a nearly billion year hiatus is further testament to the climatic extremes of the period.

It appears that the dramatic changes in ocean chemistry during the Cryogenian are not only contemporaneous with global ice ages but also with the evolution of complex life. Cohen et al. (2011) found phosphate-synthesizing microfossils within shale and carbonate facies of the Fifteenmile Group. These fossils are similar to other fossil assemblages reported by earlier workers in the region (Allison, 1980; Allison and Awramik, 1989) and may represent early taxonomic associations with Green Algae (Macdonald et al., 2010b, Cohen et al., 2011). Currently, these fossils have stratigraphic age control between about 717-811Ma (Macdonald et al., 2010b) making them roughly

150 Ma older than recognition of diverse biomineralization and coeval with reports suggestive of mineralization in vase-shaped microfossils (Porter, 2011; Porter and Knoll, 2000; Porter et al., 2003). Application of the Re-Os geochronometer to the beds in which these microfossils are documented can confirm earlier suggestions that the evolutionary record of these complex organisms needs to be extended.

One of the key limitations facing workers throughout the Cryogenian is the paucity of isotopically datable material from successions. The lack of lack of age control leaves those working in the Neoproterozoic to correlate units regionally and globally in yard-stick fashion using chemostratigraphic and lithostratigraphic based correlations. These methods are problematic due to diagenesis and lateral facies variability. Given that the Cryogenian period has great importance in deconvolving the interplay between climate, tectonics, and the evolution of life, there is substantial need for absolute radiometric age control. The development of the  $^{187}\text{Re}$ - $^{187}\text{Os}$  isotope chronometer in organic-rich mudstones has significantly expanded the amount of datable material in the Neoproterozoic. The Coal Creek Inlier represents one of the best calibrated Cryogenian data sets to date, yet it has only two age constraints for ~3km of published measured section (Macdonald et al., 2010; Macdonald et al., 2012 in press). The two age constraints of  $717.43 \pm 0.14$  Ma and  $811.5 \pm 0.1$  Ma (U-Pb in zircon, ID-TIMS, Macdonald et al., 2010a) are an excellent benchmark by which to measure the accuracy of Re-Os system in the Neoproterozoic.

This chapter reports new  $^{187}\text{Re}$ - $^{187}\text{Os}$  isotope chronology data from the Upper Reefal Assemblage of the Fifteenmile Group, Coal Creek Inlier, Yukon Territory and provides insights into the systematics of Re-Os data sets as well as the implications of new absolute chronology for the Bitter Springs isotopic stage and the evolution of complex life.

### **Methods:**

Samples were collected from 6 different shale horizons in the Fifteenmile Group of the Coal Creek Inlier. Figure 6 shows the locations of sampled ORMs and indicates which sampled sets have associated Re and Os measurements. Between 3 and 15 sample suites were taken from each unit as part of a measured section profile, enabling easy correlation with other litho- and chemostratigraphic datasets from the outcrop. Each sample suite contains between 4-6 samples. To prevent variability in initial  $^{187}\text{Os}/^{188}\text{Os}$  ratios between samples, special care was taken to select samples within the same vertical horizon. To minimize the possibility of metals contamination all samples were collected without exposure to metals, such as rock hammers. Best efforts were made to sample from fresh surfaces by digging out samples from as deep as possible within the outcrop. However, the nature of sample localities often prevented the collection of truly fresh shale samples. Figure 7 shows many of the challenges associated with sampling ORM from outcrops. Getting truly fresh samples may be difficult from any outcrop sample (George et al., 2012). Pierson-Wickmann et al. (2002) show intense Re weathering profiles in outcrop samples of black shales. The typical sample sizes

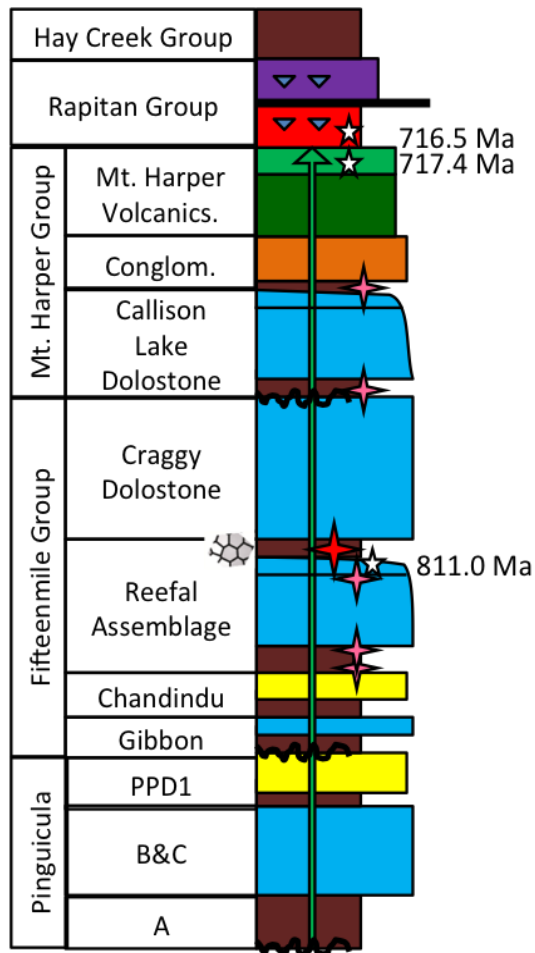


Figure 6: Stratigraphy of the Coal Creek Inlier redrawn and modified from (Halverson et al., 2011). Pink stars indicate ORMs sampled for Re-Os work. Red star shows stratigraphic position of Re-Os data set described in this work.

retrieved from the outcrop were >100 grams. Sample morphology was varied, from a solid piece about the size of a deck of cards to a group of fragmented chips less than the size of a quarter. Samples ranged in color from dark black to light grey. In some instances slight laminations were noted during sample collection. All samples were placed into marked plastic bags, recorded in a field notebook, and grouped according to sample suite during collection. The following work presents Re-Os results from the

Upper Reefal Assemblage of the Fifteenmile Group, shown as a red star in Figure 6.

All ORM were processed according to standardized digestion procedures (Selby and Creaser, 2003) and analyzed standardized analytical methods (Creaser et al., 1991;

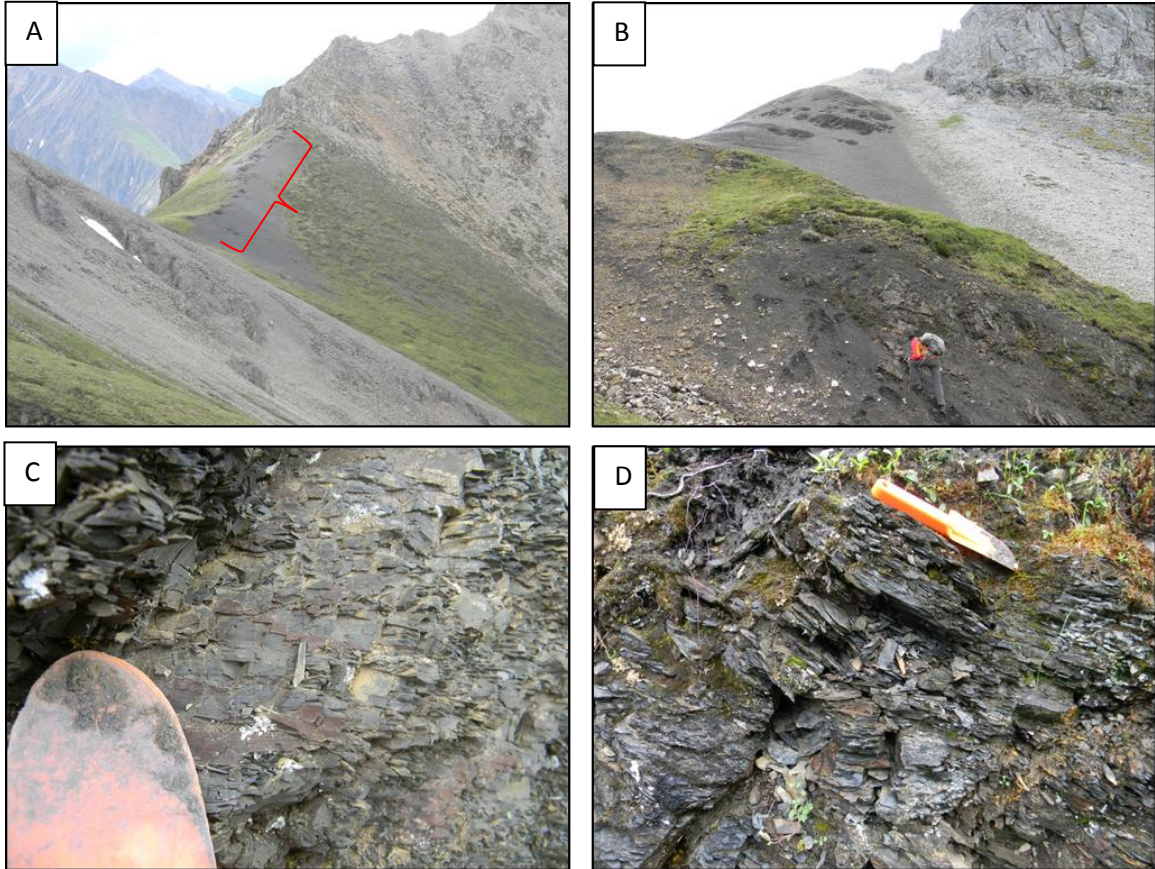


Figure 7: Field photos showing sampling difficulties in the Fifteenmile Group, Coal Creek Inlier, Yukon Territory. A) Location of Upper Reefal Assemblage and Re-Os data presented in this thesis (red star in Figure 6). The ORM horizon is well exposed but does have significant plant cover. B) The grassy cover is the approximate location of a basalt sill in the shale member of the Callison Lake Dolostone. For scale, Erik Sperling is about 2m tall. C) Small scale fracturing of well indurated ORM horizon within Upper Reefal Assemblage shown in photo A. Care must be taken to avoid these areas as they may be prone to Os<sub>i</sub> heterogeneity. Orange trowel head is ~2.5 inches wide. D) Photo shows intense fracturing and weathering of ORM outcrops in the Lower Reefal Assemblage. Orange trowel is about 10 inches in length.

Volkening et al., 1991). All sample digestion procedures were performed in hepa-

filtered, metal-free clean labs at the University of Houston and the University of Alberta under the direction of Professor Alan Brandon and Professor Robert Creaser. Sample measurements were made on a thermal ionization mass spectrometer in negative mode on a Triton-Plus at the University of Houston and a Micromass Sector54 at the University of Alberta. Blanks and standards were run during the process to ensure data accuracy and reproducibility. Total procedural blanks for reported data are between 0.3 and 1.2 ppt for Os and between 32 and 36 pg for Re. All data are presented with  $2\sigma$  errors based on the combined propagation of blank abundances, spike calibration, and reproducibility of standard analyses.

## **Results:**

### *Upper Fifteenmile Group Results*

The Re-Os results for samples from the Upper Fifteenmile Group (S11-9 and S11-15) are presented in Table 2. All of the S11-9 samples are enriched in Re (~2-8 ppb) and Os (60–200 ppt) compared to typical continental crust values (0.2–2 ppb for Re and 0.03–0.05 ppb for Os; Esser and Turekian, 1993; Peucker-Ehrenbrink and Jahn, 2001). Compared to S11-9 samples, S11-15 samples are typically less enriched in Re and Os and yield total Re and Os levels similar to crustal values (Re ~0.76-1.4 ppb and Os ~ 27-35 ppt). These samples have Re and Os levels which are similar to or less enriched than other similar age Cryogenian shales (Re ~2-500 ppb and ~Os 50 ppt-1.5 ppb: Rooney et al, 2011; Zhu et al, 2012). The  $^{187}\text{Re}/^{188}\text{Os}$  and  $^{187}\text{Os}/^{188}\text{Os}$  ratios of both sample sets

Sample	Re ppb	± 2s	Total Os ppt	± 2s	187Re/188 Os	± 2s	187/188 Os	± 2s	rho	Re % blank	187Os %/blk	188Os %/blk	Osi @750Ma	Model Age @Osi 0.4
S11-9A	6.70	0.03	172.4	1.0	301.9	1.8	4.812	0.02	0.59	0.44	0.02	0.5	1.017	871
S11-9C	2.36	0.02	61.9	0.7	283.6	3.9	4.320	0.07	0.67	2.36	0.07	1.6	0.754	824
S11-9D	5.55	0.03	110.4	1.0	420.5	4.0	5.767	0.06	0.57	0.50	0.03	0.9	0.480	761
S11-15A	1.27	0.01	-	-	-613.2	-22.3	-	-	-	2.12	-	-5.3	-	-
S11-15B	0.76	0.01	31.7	0.4	158.7	4.0	2.999	0.06	0.67	4.11	0.18	2.7	1.004	975
S11-15C	1.24	0.01	28.7	0.4	319.1	7.9	4.223	0.10	0.82	2.48	0.15	3.2	0.210	715
S11-15D	1.04	0.01	29.2	0.4	231.1	5.8	2.819	0.06	0.78	3.24	0.21	3.0	-0.087	625
S11-9A	6.33	0.01	183.9	0.8	257.1	2.2	4.346	0.04	0.74	0.78	0.07	1.0	1.113	914
S11-9C	2.43	0.01	61.5	0.4	288.8	6.7	4.082	0.09	0.86	2.10	0.22	3.0	0.450	760
S11-9D	5.54	0.01	102.4	0.6	469.6	7.2	6.265	0.09	0.94	0.92	0.10	2.2	0.360	745
S11-15B	1.27	0.01	35.4	0.2	239.7	6.5	3.052	0.07	0.84	2.86	0.34	3.4	0.038	660
S11-15C	1.38	0.01	29.4	0.3	358.1	16.2	4.607	0.19	0.91	3.48	0.40	6.2	0.105	701
S11-15D	1.09	0.01	27.6	0.3	266.5	14.7	3.174	0.15	0.86	5.38	0.68	7.2	-0.177	621
S11-9a B1	7.55	0.03	196.6	1.4	295.3	2.0	4.691	0.03	0.65	0.70	0.03	1.3	0.978	866
S11-9c B1	2.73	0.02	86.7	0.7	210.8	2.3	3.126	0.03	0.71	1.86	0.09	2.5	0.476	771
S11-9d B1	8.22	0.03	205.6	1.0	258.2	1.4	2.738	0.01	0.59	0.64	0.04	1.1	-0.509	541
S11-9a B2	7.48	0.03	200.2	1.2	289.1	1.6	4.668	0.02	0.63	0.66	0.03	1.2	1.033	880
S11-9c B2	2.71	0.02	103.5	0.7	164.9	1.6	2.464	0.02	0.65	1.95	0.10	2.1	0.390	746
S11-9d B2	5.90	0.03	120.6	1.0	411.6	3.5	5.858	0.05	0.81	0.89	0.05	2.3	0.684	791

Table 2: Re and Os results from ORMs in the Upper Reefal Assemblage, Coal Creek Inlier. Data are bracketed by analytical session. Data with blue headers were collected at the University of Alberta and data with red headers were collected at the University of Houston. All data are presented with 2σ errors calculated from propagation of blank, measurement, and standard uncertainty.

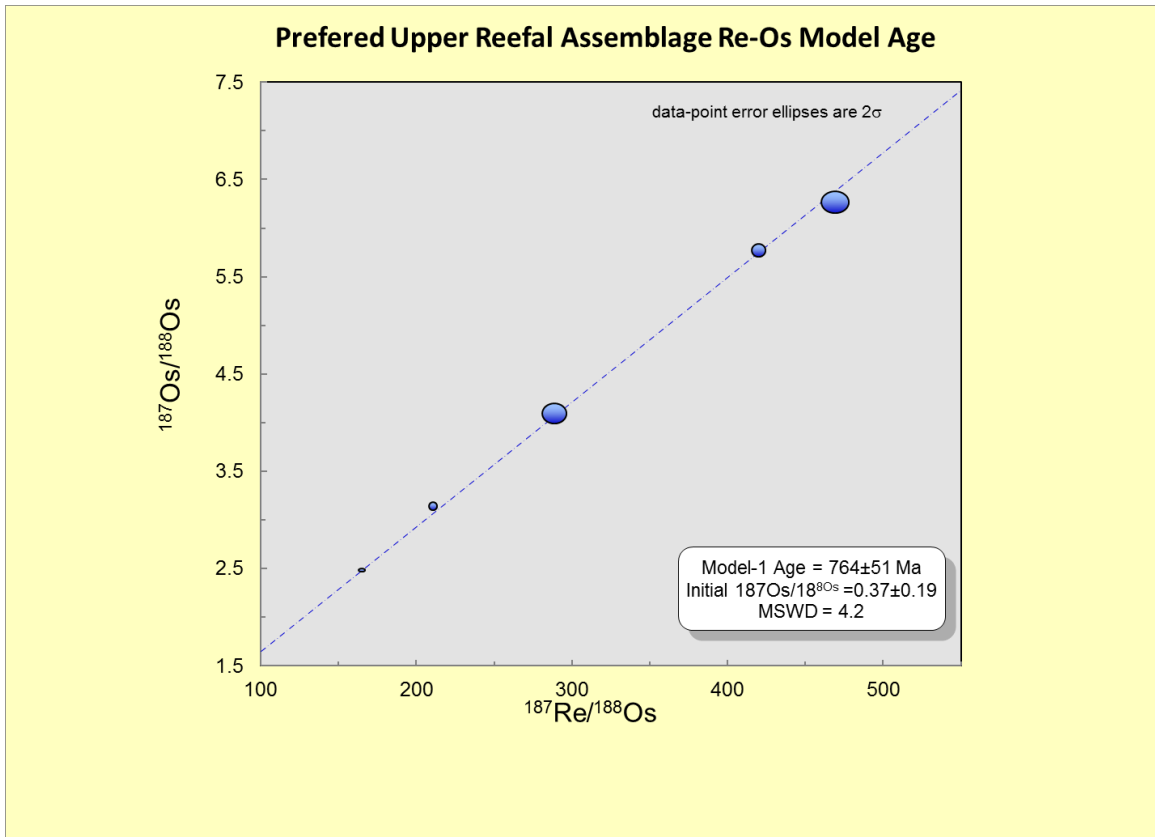


Figure 8: Preferred Re-Os depositional Model-1 age of the Upper Reefal Assemblage, Coal Creek Inlier, Yukon Territory. Isochron calculated and plotted using *Isoplot 4.15* (Ludwig, 2008).

vary from ~150-470 and ~2.4-6.2 respectively and are positively correlated with each other. The uncertainty in Re and Os abundance varies from 0.1–1.6%, 0.2–1.5%. The uncertainty of  $^{187}\text{Re}/^{188}\text{Os}$  and  $^{187}\text{Os}/^{188}\text{Os}$  varies from 0.46–5.5% and 0.39–4.8% respectively. The calculated  $\text{Os}_i$  @750 Ma of S11-9 and S11-15 samples ranges from – 0.509 to 1.113.

Isochrons for the S11-9 and S11-15 sample sets were calculated using the *Isoplot 4.15* macro for excel (Ludwig, 2008). The software uses the accepted decay constant of  $^{187}\text{Re}$  decay constant of  $1.666 \times 10^{-11} \text{ year}^{-1}$  (Smoliar et al., 1996). All samples from the

Upper Fifteenmile Group plot along an isochron with a Model-3 age solution of  $752 \pm 180$  Ma ( $2\sigma$ ; MSWD 529;  $O_{Si}$   $0.46 \pm 0.91$ ). Samples from just the S11-9 horizon plot along an isochron with a Model-3 solution of  $758 \pm 210$  Ma ( $2\sigma$ ; MSWD 775;  $O_{Si}$   $0.6 \pm 1.1$ ). The S11-9a samples plot along an isochron with a Model-3 age solution of  $610 \pm 69$  Ma ( $2\sigma$ ; MSWD 2.6;  $O_{Si}$   $1.71 \pm 0.34$ ). The 9c and 9d sample subset plots along a Model 3 Re-Os age of  $795 \pm 210$  Ma ( $2\sigma$ ; MSWD 732;  $O_{Si}$   $0.1 \pm 1.1$ ). Excluding a sample with a negative  $O_{Si}$  and two samples with elevated  $O_{Si}$ , data from the 9c and 9d subset plot along an isochron with a Model-1 age of  $764 \pm 51$  Ma ( $2\sigma$ ; MSWD 4.2;  $O_{Si}$   $0.37 \pm 0.19$ ). Figure 8 shows the isochron diagram for the 9c and 9d data set using a Model-1 age solution. Calculating a Model-3 solution from the same data set results in a model age of  $752 \pm 44$  Ma ( $2\sigma$ ; MSWD 4.2;  $O_{Si}$   $0.42 \pm 0.22$ ). These data points show no correlation between  $1/O_{S_{total}}$  and  $^{187}Os/^{188}Os$ . Excluding a data point with high  $O_{Si}$ , samples from the stratigraphically lower S11-15 horizon of the upper Fifteenmile group plot along an isochron with a Model-3 age solution of  $892 \pm 100$  Ma ( $2\sigma$ ; MSWD 1.8;  $O_{Si}$   $-0.61 \pm 0.44$ ).

## Discussion:

### *Differences between Laboratories*

The Re-Os laboratories at the University of Houston and at the University of Alberta under the direction of Professor Alan Brandon and Professor Robert Creaser respectively produced the data reported in this thesis. In order to ensure data equivalence the data are compared with each other to ensure there are no systematic differences between data reported from the laboratories. Figure 9 shows the differences between Re and Os measurements at the two laboratories. There do appear to be some systematic differences between the UH and UA laboratories in the amount total Re and Os measured. The UH laboratory measures higher amounts of total Re and total Os in all samples compared to UA. This could be indicative of slightly better yields at the University of Houston. When comparing differences in the measured  $^{187}\text{Re}/^{188}\text{Os}$  vs.  $^{187}\text{Os}/^{188}\text{Os}$  ratios, the two laboratories replicate each other with the exception of the S11-9c samples and an anomalous measurement of sample 9d. The anomalous measurement of sample 9d is easy to distinguish from the other samples by its negative  $\text{Os}_i$  and has a total measured Os nearly twice that of the other three 9d analyses. This could indicate contamination of the sample or inadequate sample-spike equilibration. Despite the differences between laboratories in the measured isotopic ratios, three of the four S11-9c samples from both laboratories have similar  $\text{Os}_i$  values: 0.450, 0.476, and 0.390. This is suggestive that the differences between laboratories may be related to sample heterogeneity rather than quantitative differences between laboratories. The

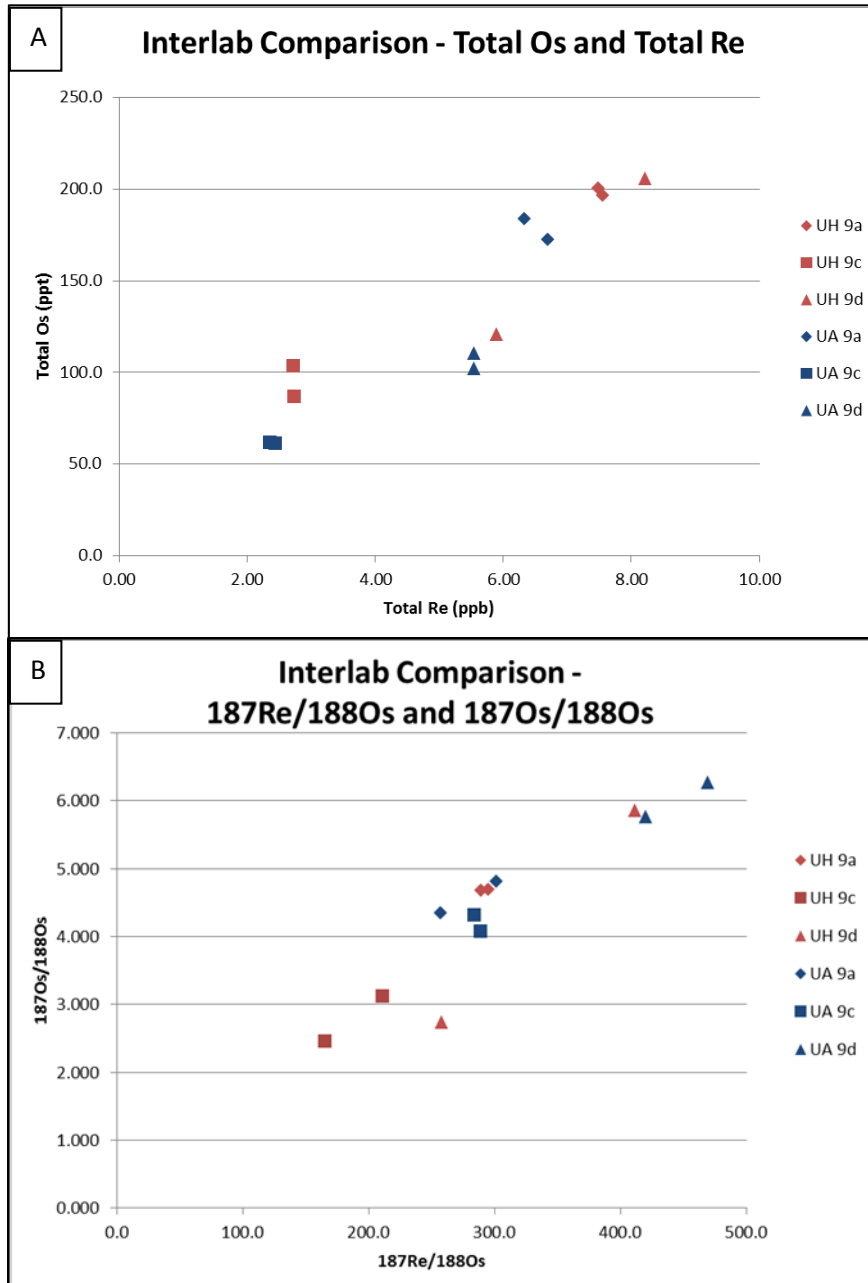


Figure 9: Inter-laboratory comparison of A) total Re and Os measured as well as B)  $^{187}\text{Re}/^{188}\text{Os}$  and  $^{187}\text{Os}/^{188}\text{Os}$  ratios. For implications see discussion.

lack of material differences between the data gathered from the two laboratories suggests that the data can be merged without fear of mixing incomparable data.

#### *Heterogeneity in $Os_i$ in samples from the Fifteenmile Group*

Initial  $Os$  ratio heterogeneity is a primary source of geologic scatter in the Re- $Os$  chronometer. Due to the relatively short residence time of  $Os$  in seawater  $\sim 5$ -40 ky (Pegram et al., 2002 and Oxburg et al., 2007) and the typical low rates of deposition in ORMs, variation in  $Os_i$  can occur with small vertical stratigraphic displacement (Cohen et al., 1999). A principle method to minimize complications from natural  $Os_i$  variation utilizes a sampling strategy that selects samples from a single continuous horizontal stratigraphic horizon. However, this method of sampling strategy can be difficult to implement in areas that are poorly exposed, contain microscale structure, or are intruded by sills and dikes (e.g. Figure 7). Despite these impediments to sampling, every effort was made to obtain fresh samples from continuous horizons.

Another issue that leads to apparent  $Os_i$  variability is post depositional alteration of the samples. Alteration can take many forms including gain or loss of  $Os$  and/or Re due to fluxing of hydrothermal fluids or meteoric water as well as chemical weathering of exposed samples (Peucker-Ehrenbrink and Hannigan, 2000; Jaffe et al., 2002; Georgiev et al., 2012). The chemical weathering profile of  $Os$  and Re can extend  $\sim 5$ m beneath the exposed surface (Pierson-Wickmann et al., 2000; Jaffe et al., 2002). Unlike other works, which take advantage of fresh samples thanks to road cuts or core

samples, which are exposed for geologically minuscule amounts of time, the rocks studied in the Coal Creek Inlier may have been exposed since the last glaciers receded from the area. However, on a qualitative scale the effect of weathering on the rocks in the Yukon is thought to be less than would have occurred in temperate or tropical regions (Forsberg and Bjoroy, 1983; Littke et al., 1991). Due to the remoteness of the region and the induration of the ORMs sampled, it was not possible to dig far enough into the outcrop to obtain truly fresh samples. Therefore in order to minimize contamination samples analyzed were selected because of their cohesiveness, lack of visible fracture, and evidence of surface oxidation (orange to rust colored rind). However, recent work (Georgiev et al., 2012) suggests that even best efforts to control for these factors can still result in outcrop samples that are not isochronous.

Model age solutions with extremely positive or negative  $O_s$  as well as high MSWD's can be indicative of altered data sets (Yang et al., 2009; Ronney et al., 2010). Since Re and Os are both known to be disproportionately enriched in ORMs compared to crustal averages (Peucker-Ehrenbrink and Hannigan, 2000; Peucker-Ehrenbrink and Ravizza, 2000), samples that are not enriched in Re and Os relative to crustal averages may also indicate loss of Re and Os due to weathering. Both the S11-9 and S11-15 sample sets have considerable evidence of disturbance. When considering the S11-9 sample set as a group, the model age is consistent with known U-Pb age constraints, but yields an extremely high MSWD (>700) and has very large errors (210Ma;  $2\sigma$ ) on both the model age and  $O_s$  (1.1;  $2\sigma$ ) which is suggestive of disturbance. Further, the S11-9a

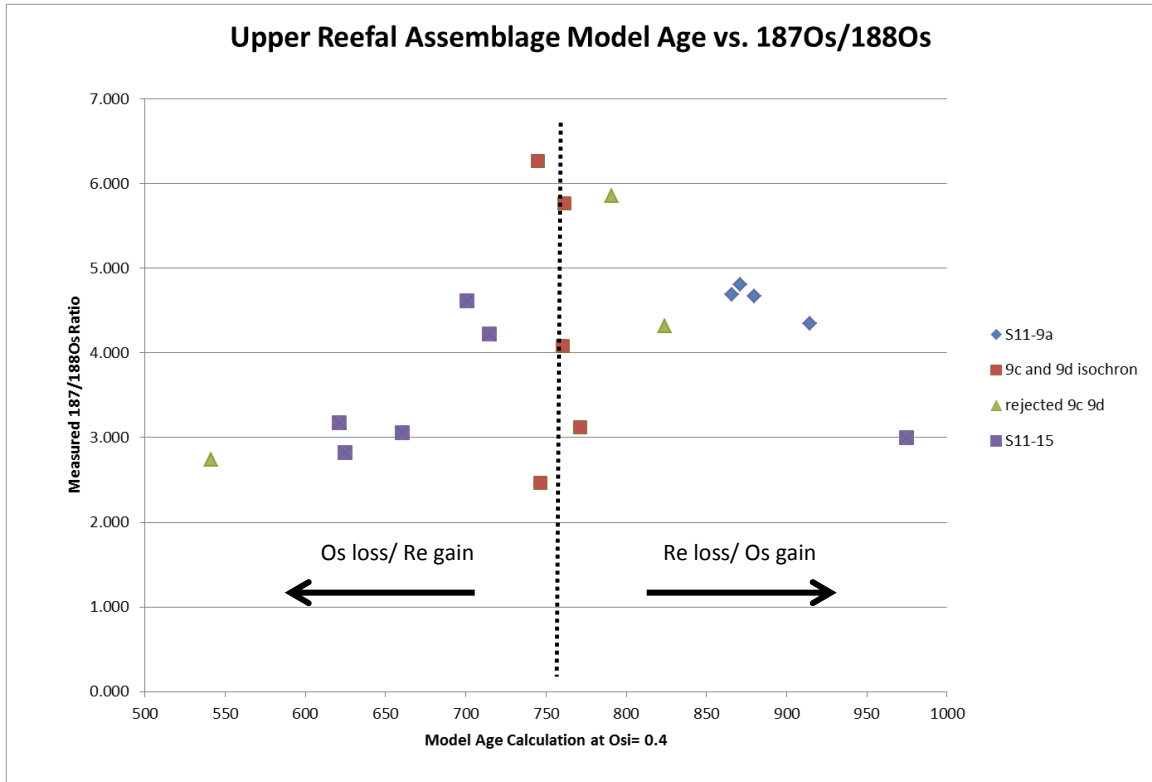


Figure 10: Weathering discrimination diagram after Georgie et al. (2012). Arrows suggest Re loss/Os gain and Os loss/Re gain respectively. The dashed vertical line shows an idealized distribution. S11-9a samples appear to have lost Re/gained Os whereas S11-15 samples appear to have lost Os/gained Re.

data set plots along a trend towards a very radiogenic  $Os_i$  (1.7) value. Data sets that plot to very radiogenic values have been shown to be disturbed by hydrothermal weathering alteration (Kendal et al., 2009). However, the calculated  $Os_i$  of the S11-9a samples as well as the calculated model ages suggest these samples are may have lost  $^{187}Re$  making them appear older. Figure 10 uses Upper Fifteenmile Group data to populate a discrimination diagram developed by Georgiev et al. (2012). This discrimination diagram also suggests that the S11-9a samples lost  $^{187}Re$ . Furthermore, no basalt sills or dikes are reported in the vicinity of the Upper Fifteenmile samples analyzed here. Based on both the chemistry of the data set and the lack of evidence for hydrothermal alteration it

appears the scatter in the S11-9 data set is the result of chemical weathering. Similarly, the S11-15 samples when plotted as a group yield an isochron with a negative  $Os_i$  ( $-0.6 \pm 0.44$ ), an age older than known age constraints, and systematically have total Os and Re abundances that are not enriched compared to average crustal values. These three factors taken together are suggestive of significant alteration. Therefore, this work favors the assessment that the heterogeneity in  $Os_i$  of the S11-9a and S11-15 sample suites is due to post-depositional alteration, much of the disturbance may be attributable to varying degrees of chemical weathering.

However, this work considers the Model-1 age of  $764 \pm 51$  Ma ( $2\sigma$ ; MSWD 4.2;  $Os_i$   $0.37 \pm 0.19$ ) calculated from the S11-9c and 9d sample suite a robust age for the deposition of the Upper Fifteenmile group. Unlike other portions of the sample suite, the data used to create this isochron did not show significant variation in calculated  $Os_i$  ( $0.360$  and  $0.480$ ), compared to  $-0.509$ - $0.754$  for all of 9c and 9d, and compared to all sample 9 data between  $-0.509$ - $1.112$ . The samples also show the small spread in calculated model ages ( $744$ - $771$ Ma) compared to ( $541$ - $824$ Ma) for all 9c and 9d and ( $541$ - $914$ Ma) for all of S11-9. The coherency these data points suggest that they represent the unaltered or least altered group of analyses in the data set. Therefore, this work considers the Model-1 age of  $764 \pm 51$  Ma ( $2\sigma$ ; MSWD 4.2;  $Os_i$   $0.37 \pm 0.19$ ) calculated from the S11-9c and 9d sample suite a robust age for the deposition of the Upper Fifteenmile group.

### *Significance of the Re-Os Depositional Age of the Fifteenmile Group*

The depositional age of the Upper Fifteenmile Group in the Coal Creek Inlier provides important absolute age control for multiple processes and events with global significance. The age provides age control for the same horizon from which some of the earliest known mineralizing algae are reported (Macdonald et al. 2010; Cohen et al., 2011). This age also provides valuable age control for correlation to other radiometric age data from the region (e.g. Bergman et al., 1993 unpublished data; Macdonald et al., 2010; VanAcken et al., 2012), and provides direct control for a globally recognized carbon isotope excursion known as the 'Bitter Springs' stage (Halverson, 2007; Jones et al., 2010; Macdonald et al., 2010b).

The depositional age of  $764 \pm 51$  Ma ( $2\sigma$ ; MSWD 4.2;  $Os_i$   $0.37 \pm 0.19$ ) for the Upper Fifteenmile group provides confirmation of previous work, which suggests stratigraphic age control between  $811.5 \pm 0.2$  Ma and  $717.4 \pm 0.1$  Ma by U-Pb ID-TIMS on zircons (Macdonald et al., 2010; Cohen et al., 2011). The relatively large error ( $\sim 6.5\%$ ) of the Re-Os determination prevents a more precise definition of the age of these fossils than previous workers were able to estimate. However the confirmation of the Cryogenian age for these early biomineralizers suggests that the fossil record of biomineralization must be significantly extended from the earlier suggestions of latest Ediacaran appearance (Germs, 1972; Grotzinger et al., 2000).

The depositional age for the Upper Fifteenmile group also has significant ramifications for the development of absolute chronology-based stratigraphy in Cryogenian age sections of northwest Canada. Considering previously published ID-TIMS ages (Macdonald et al., 2010), new Re-Os ages (VanAcken et al., 2012), unpublished zircon fission track ages (Bergman et al. 1993: data courtesy of first author), and the  $^{187}\text{Re}$ - $^{187}\text{Os}$  isotope ages presented in this work, the absolute chronology of the Cryogenian sections across a 1500km section from Alaska to Canada is well constrained. Figure 11 shows a schematic correlation of these sections from Alaska to Canada. Absolute  $^{187}\text{Re}$ - $^{187}\text{Os}$  isotope chronology from these works correlates the Upper Shale horizon of the Fifteenmile Group in the Coal Creek Section ( $764 \pm 51 \text{ Ma } 2\sigma$ ; this work), the Upper Shale horizon of the Tindir Section ( $724.2 \text{ Ma } \pm 60 2\sigma$ ; Bergman et al., 1993), and the Upper Carbonate member of the Wynniatt Fm. ( $762 \pm 46 \text{ Ma } 2\sigma$ ; van Acken et al., 2012) (See Figure 11). These ages confirm the correlations previously proposed by Macdonald et al. (2010) between the Coal Creek Inlier and the Victoria Islands the basis of a negative  $\delta^{13}\text{C}$  excursion.

The correlation based on the negative  $\delta^{13}\text{C}$  excursion also extended into the Mackenzie Mountains. The age  $^{187}\text{Re}$ - $^{187}\text{Os}$  isotope age control from Victoria Island and the Coal Creek Inlier are imply that the Upper Carbonate unit of the Little Dal Group in the Mackenzie Mountains should yield an equivalent age. However, sills and dykes cross cutting units through the Little Dal Basalt are dated to  $779.5 \pm 2.3 (2\sigma; \text{MSWD} = 0.21; \text{U-Pb in baddeleyite})$  in the Mackenzie Mountains (Harlan et al., 2003). This age is

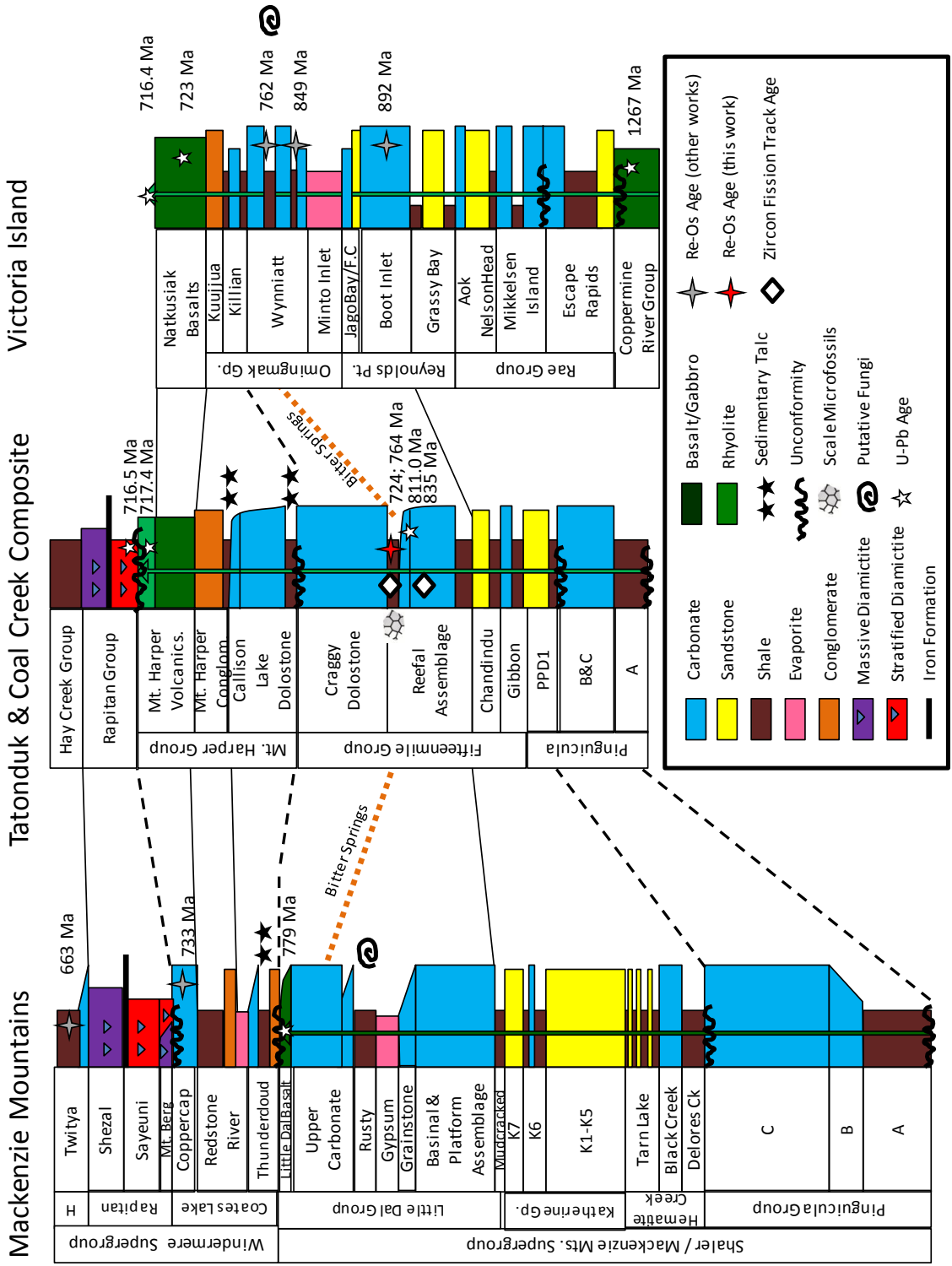


Figure 11: Correlation of Cryogenian age deposits across Alaska and Canada. Redrawn and modified from Halverson et al (2012). Stratigraphy from Aitken et al. (1981, 1989); Hoffman and Halverson (2011); Macdonald et al. (2010, 2011); Halverson et al. (2012); Rainbird et al. (1996); Jones et al. (2010). Little Dal Basalt 779 age from Harlan et al. (2003). U-Pb TIMS ages of 716.5, 717.4, 811.0, 716.4 Ma from Macdonald et al., (2010). Natkusiak Basalt 723 age from Heaman et al. (1992). Coppermine River Group 1267 age from LeCheminant and Heaman (1989). Mackenzie Mountains Re-Os ages from Rooney et al (2011). Victoria Island Re-Os ages from VanAcken et al. (2012). Coal Creek Re-Os ages are from this work. Zircon fission track ages are from Bergman et al. (1993; unpublished). Orange dashed line shows correlation of the Bitter Springs stage. Black dashed lines are inferred correlations of unconformities and solid black lines are inferred correlations from Halverson et al. (2012).

problematic because these dyke swarms are interpreted to cross cut the negative  $\delta^{13}\text{C}$  excursion, which in correlated sections has a younger age  $\sim 760\text{Ma}$  (this work and VanAcken et al., 2012). The large errors  $\pm 6\%$  or  $\sim 50\text{Ma}$  on both Re-Os ages prohibits definitively confirming an age younger than  $\sim 779\text{Ma}$  for the negative  $\delta^{13}\text{C}$  excursion.

The negative  $\delta^{13}\text{C}$  excursion is known as the Bitter Springs isotopic stage and is age equivalent across the Alaskan-Canadian Cryogenian section. The age equivalence of the section supports work which suggests the global nature of the Bitter Springs Stage (Hill et al., 2000; Halverson et al., 2005; Halverson et al., 2007; Swanson-Hysell et al., 2010; Halverson and Shields-Zhou, 2011). Halverson et al. (2007) has speculated that the origin of the anomaly could be an unrecognized glacial event. Whereas recent work by Swanson-Hysell et al. (2011) builds upon ideas constructed in Maloof et al. (2006) that suggest anomalous paleomagnetic signatures from within the Bitter Springs isotopic stage record true polar wander events, which could trigger disturbances in the carbon isotope record. Despite evidence for a true polar wander event during the Bitter Springs, Swanson-Hysell et al. (2011) were unable to confirm the true polar wander event, instead suggesting it as an intriguing possibility deserving more research. One reason Halverson et al. (2007) may have been unable to identify a glacial event significant enough to produce the global anomaly is the assumption of a circa  $800\text{Ma}$  age for the Bitter Springs isotopic stage. The data presented here along with other recently obtained radiometric constraints suggest the Bitter Springs Stage in Cryogenian sections of Alaska-Canada is more likely circa  $760\text{Ma}$ . This younger age may also lead to

important revisions for those reconstructing paleogeographies based on paleomagnetic records from the Bitter Springs Stage.

One possibility posed new radiometric control for the Bitter Springs stage (~760Ma) is a correlation with the Kiagas Glaciation. The Kiagas Glaciation is named for glacial diamictites found in Southern Namibia and South Africa (Rodgers, 1916; Beetz, 1926). The age of the glacial diamictites in the Kiagas Fm. are constrained to a maximum of  $771 \pm 6$  Ma ( $2\sigma$ ; Frimmel et al., 2001) based on U-Pb zircon ages from the granitic basement on which the Kiagas Fm. sits. The Kiagas is constrained to a minimum of  $752 \pm 6$  Ma (Borg et al. 2003) and  $741 \pm 6$  Ma (Frimmel et al., 1996) based on U-Pb and Pb-Pb ages from zircons respectively. Frimmel (2011) suggests these deposits could represent a period global glaciation. There is evidence of a glacial sequence and cap carbonate in the Sete Lagoas member of the Bambuí Group of the São Francisco basin, Brazil (Vieira et al., 2007). The authors find that the chemostratigraphic record of the glacial event does not match with the assumed Sturtian glacial horizon. Further work by Babinski et al. (2007) obtained a Pb-Pb isochron age from the cap carbonate on top of the glacial units, obtaining an age of  $740 \pm 22$  Ma. Further, hydrothermal zircons ( $748 \pm 3$  Ma) occur within granites in the Dabie–Sulu orogenic belt, China that have anomalously low  $d^{18}\text{O}$  values (Zhang et al., 2007). Despite experiencing ultrahigh pressure metamorphism (~800°C and ~3.3 GPa), one possible explanation for the low  $\delta^{18}\text{O}$  values in the granites is interaction with meteoric water from a cold paleoclimate. While this evidence is not enough to confirm a pan-glacial event during the Bitter Springs Stage, it is enough to be

speculative of a possible correlation between the Bitter Springs and the Kiagas age glaciation. Further refinement and an improvement in the accuracy of  $^{187}\text{Re}$ - $^{187}\text{Os}$  isotope age control from this and other Bitter Springs horizons could improve evidence for a link between the negative carbon isotope excursion and Kiagas age glacial events across the globe.

If improved age resolution finds the Kiagas and Bitter Springs are coeval, it has significant implications for glacial events in the Cryogenian. Many workers have argued that Cryogenian glaciations represent global glaciations to low latitude (e.g. Hoffman et al., 1998). But, overlapping glacial and non-glacial horizons during a Kiagas – Bitter Springs event would argue for localized glaciation, where glacial events responded to regional draw-down of  $\text{CO}_2$  related to rifting of Rodinia (Eyles and Januszczak, 2004). This would imply the possibility of at least 2 glacial styles during the Neoproterozoic and is suggestive of a more complex climatic regime in the Cryogenian.

### **Conclusions:**

(1) This work presents a new  $^{187}\text{Re}$ - $^{187}\text{Os}$  isotope depositional age for the Upper Fifteenmile Group  $764 \pm 51$  Ma ( $2\sigma$ ; MSWD 4.2;  $\text{Os}_i$   $0.37 \pm 0.19$ ) (2) This age confirms previous work which assigns the evolution of early biomineralizing eukaryotes to the Cryogenian (3) Identical  $^{187}\text{Re}$ - $^{187}\text{Os}$  isotope ages from Victoria Island, Canada and the Coal Creek Inlier, Yukon Territory, Canada confirm correlations based on the  $\delta^{13}\text{C}$  (4) This work reassigns the age of the Bitter Springs from  $\sim 800$  Ma to  $\sim 760$  Ma on the basis

of two identical  $^{187}\text{Re}$ - $^{187}\text{Os}$  isotope ages. (5) A speculative correlation between the Kiagas Glaciation and the Bitter Springs Stage is proposed on the basis of time equivalence. Improved precision in  $^{187}\text{Re}$ - $^{187}\text{Os}$  isotope and other radiometric dating tools is needed to test this correlation.

## **Chapter 3: Preliminary Re-Os Geochronology of the Quamby Mudstone, Turnbridge**

### **Borehole, Tasmania**

#### **Introduction:**

Recent work on the late Paleozoic Ice Age The Turnbridge Borehole, Tasmania records the signatures of cyclic glacial periods in the Parmeener Supergroup spanning the late Carboniferous- early Permian (Fielding et al., 2010). Figure 12 shows the location of the Turnbridge Borehole as well as schematic stratigraphy of the region. Early biostratigraphic work suggested the Woody Island Formation's basal member, the Quamby Mudstone, is earliest Permian (Clarke and Farmer, 1976). Recent work biostratigraphic work assigns the base Quamby Mudstone to the Sakmarian (~293 Ma; Henry et al., 2012). The only available radiometric age control for the Parmeener Supergroup are detrital zircon ages, which provide a maximum depositional age of Late Triassic for the quartz sandstones in the Upper Parmeener Supergroup (Rozefelds et al., 2011). In order to better constrain the timing of glacial cyclicity and transition in the Lower Parmeener Supergroup, ORM samples from the Quamby Mudstone are analyzed for Re-Os geochronology.

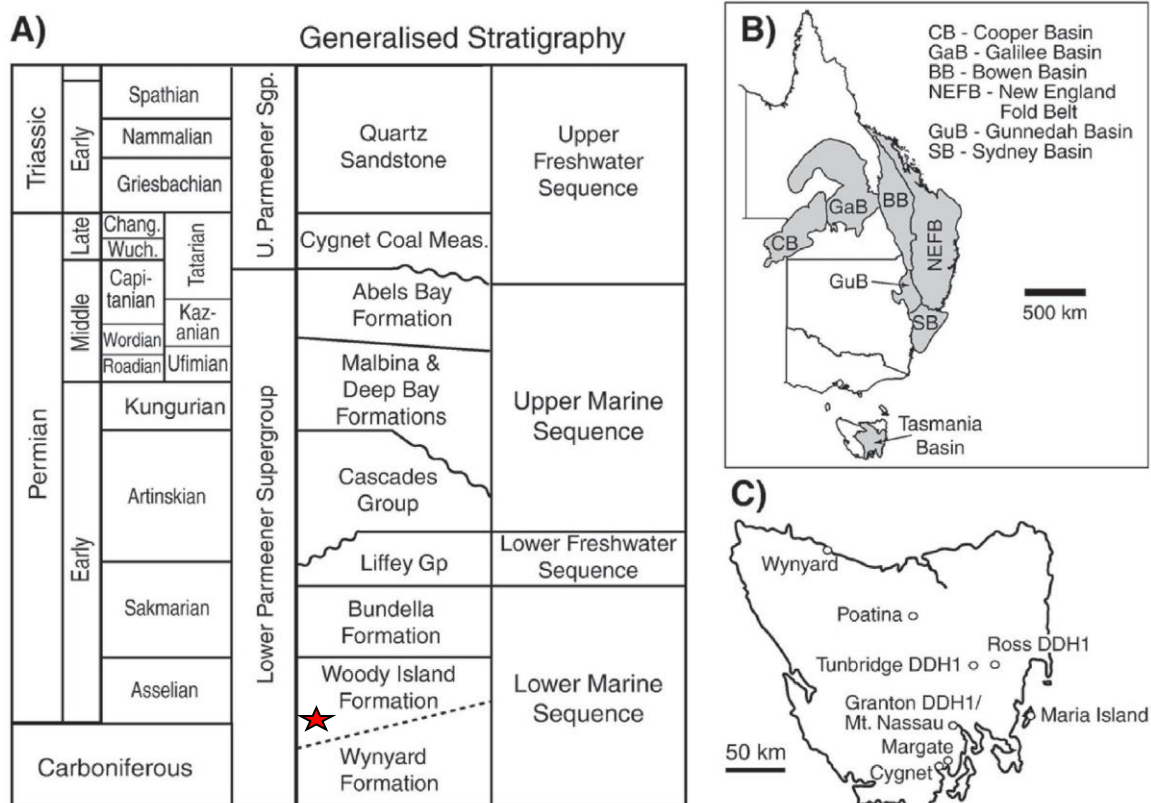


Figure 12: From Fielding et al. (2010). A) Generalized stratigraphy of the Parmeener Supergroup B) Australian basins with correlated stratigraphy. C) Locations of outcrops and boreholes which expose the Parmeener Supergroup. Note the location of the turnbridge borehole. Red star indicates approximate level of Re-Os samples reported in this work.

### Methods:

Two ~3 inch long 2.5 inch diameter core plugs were selected from the Quamby Mudstone, Turnbridge Borehole. The samples selected come from borehole depths of 674m and 701m respectively. The ~30m spread in sample depths has the potential to increase error in the Re-Os method if there is significant variation in the Os<sub>i</sub> between the two samples. The 674m core plug was cut horizontally into 3 sample splits. The 701m core plug was cut horizontally into 2 sample splits. Sample splits yielded between ~70-200 grams of powdered ORM. For simplicity, the core splits from 674m are referred to

as TB-6a,b,c and the core splits from 701m are referred to as TB-7a,b in the results and discussion section. All exposed surfaces were ground and polished using silicon carbide to remove any surface weathering or drilling residue. Re and Os extraction and measurement procedures followed the analytical procedures described in Chapter 1 as well as published in Selby and Creaser (2003).

### **Preliminary Results and Discussion:**

The Re-Os results for samples from the Quamby Mudstone are presented in Table 3. All of the Quamby Mudstone samples are enriched in Re (~8-11 ppb) and Os (~150–360 ppt) compared to typical continental crust values (0.2–2 ppb for Re and 0.03–0.05 ppb for Os: Esser and Turekian, 1993; Peucker-Ehrenbrink and Jahn, 2001). The  $^{187}\text{Re}/^{188}\text{Os}$  and  $^{187}\text{Os}/^{188}\text{Os}$  ratios of both core plugs vary from ~124-328 and ~0.88-2.1 respectively and are positively correlated with each other. The uncertainty in Re and Os abundance varies from 0.37–0.39% and 0.25–0.5% respectively. The uncertainty in  $^{187}\text{Re}/^{188}\text{Os}$  and  $^{187}\text{Os}/^{188}\text{Os}$  ratios varies from 0.41–0.54% and 0.27–0.6% respectively. The calculated model age of the Turnbridge samples with an  $\text{Os}_i = 0.5$  ranged from 192 to 315 Ma.

Isochrons for the Quamby Mudstone sample set were calculated using the Isoplot 4.15 macro for excel (Ludwig, 2008). The software uses the accepted decay constant of  $^{187}\text{Re}$  decay constant of  $1.666 \times 10^{-11} \text{ year}^{-1}$  (Smolier et al., 1996). All samples from the Quamby Mudstone plot along an isochron with a Model-3 age solution of  $373 \pm 72 \text{ Ma}$

Sample	Re ppb	± 2s	Total Os ppt	± 2s	<sup>187</sup> Re/ <sup>188</sup> Os	± 2s	<sup>187</sup> / <sup>188</sup> Os	± 2s	rho	% Re blank	% <sup>187</sup> Os blk	% <sup>188</sup> Os blk	Model Age @IOs = 5
<b>TB 6a</b>	8.23	0.032	362.0	0.9	120.4	0.5	0.885	0.003	0.33	0.596	0.021	0.13	192
<b>TB 6b</b>	8.13	0.031	152.1	0.6	326.7	1.5	2.186	0.007	0.52	0.530	0.021	0.31	309
<b>TB 6c</b>	8.26	0.033	154.0	0.8	328.1	1.8	2.189	0.013	0.46	0.625	0.025	0.37	299
<b>TB 7a</b>	11.00	0.041	234.3	0.8	279.9	1.1	1.942	0.005	0.44	0.450	0.017	0.22	308
<b>TB 7b</b>	8.15	0.032	201.7	0.7	235.6	1.0	1.739	0.005	0.45	0.586	0.021	0.25	315

Table 3: Rhenium and Osmium results from Quamby Mudstone, Lower Parmeener Supergroup, Turnbridge Borehole, Tasmania

( $2\sigma$ ; MSWD 211;  $O_s$   $0.18 \pm 0.32$ ). Removing the sample TB-6a, which has a low Rho value, from the data set yields an isochron with a Model-3 solution of  $294 \pm 29$  Ma ( $2\sigma$ ; MSWD 4.2;  $O_s$   $0.58 \pm 0.14$ ).

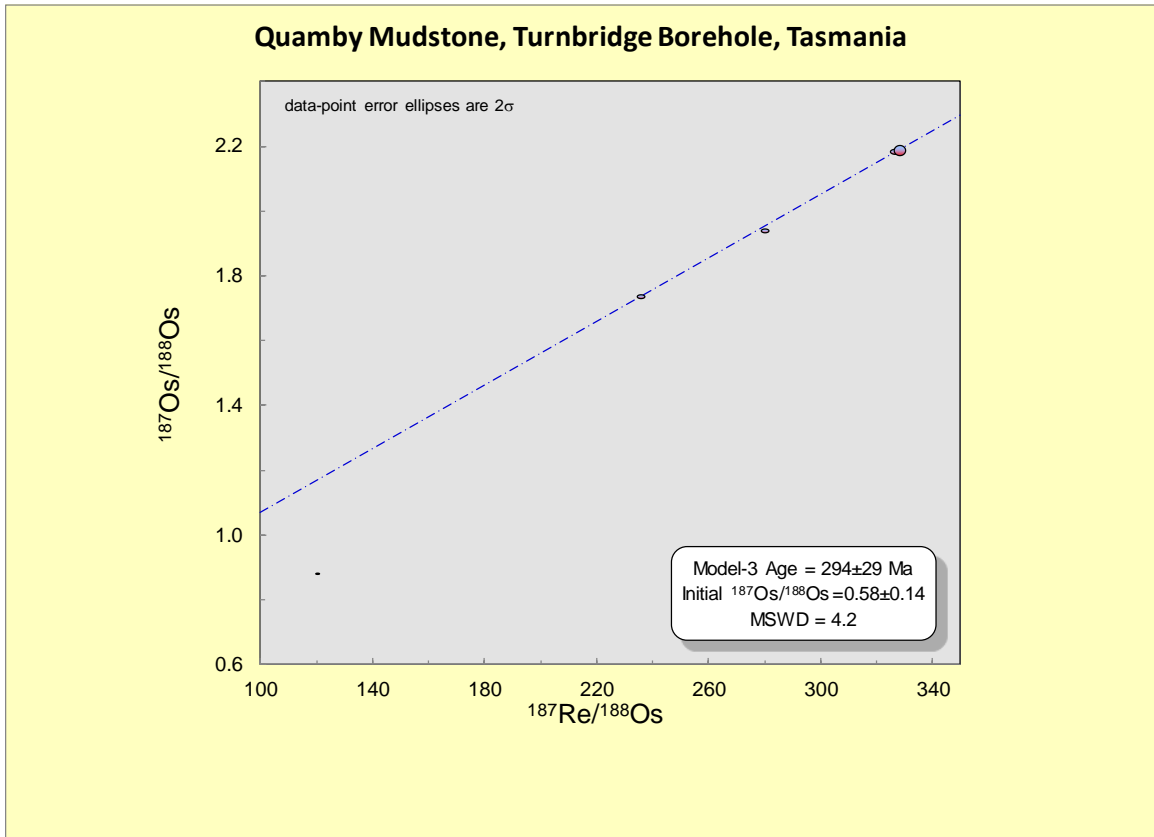


Figure 13: Preferred Isochron for the Quamby Mudstone, Turnbridge Borehole, Tasmania.

## References:

- Allison, C.W.A., 1980, Siliceous microfossils from the lower Cambrian of northwest Canada: possible source for biogenic chert. *Science*, 211, 53–55.
- Allison, C.W.A. and Awramik, S.M., 1989, Organic-walled microfossils from earliest Cambrian or latest Proterozoic Tindir Group rocks, northwest Canada. *Precambrian Research*, 43, 253-294.
- Anbar, A.D., Creaser, R.A., Papanastassiou, D.A., Wasserburg, G.J., 1992, Rhenium in seawater confirmation of generally conservative behavior. *Geochimica et Cosmochimica Acta*, 56, 4099-4103.
- Anbar, A.D., Duan, Y., Lyons, T.W., Arnold, G.L., Kendall, B., Creaser, R.A., Kauffman, A.J., Gordon, G.W., Garvin, J., and Buick, R., 2007, A whiff of oxygen before the Great Oxidation Event *Science*, 317, 1903-1906.
- Babinski, M., Vieira, L.C., and Trindade, R.I.F., 2007, Direct dating of the Sete Lagoas cap carbonate, (Bambui Group, Brazil) and implications for the Neoproterozoic glacial events. *Terra Nova*, 19, 401-406.
- Baioumy H. M., Eglinton L. B., and Peucker-Ehrenbrink B., 2011, Rhenium–osmium isotope and platinum group element systematics of marine vs. non-marine organic rich sediments and coals from Egypt. *Chemical Geology*, 285, 70–81.
- Beetz, W., 1926, Über Glazialschichten an der Basis der Nama- und Konkupformation in der Namib Sudwestafrikas. *Neues Jahrbuch f. Mineralogie, Geologie und Palaontologie, Abteilung B*, 56, 437-481.
- Borg, G., Karner, K., Buxtom, M., Armstrong, R., and Van der Merwe, S.W., 2003, Geology of the Skorpion zinc deposit, southern Namibia. *Economic Geology*, 98, 749-771.
- Brandon A. D., Norman M. D., Walker R. J., and Morgan J. W., 1999,  $^{186}\text{Os}$ - $^{187}\text{Os}$  systematics of Hawaiian picrites. *Earth Planetary Science Letters*, 174, 25–42.
- Brandon, A.D., Walker, R.J., Morgan J.W., and Goles, G.G., 2000, Re–Os isotopic evidence for early differentiation of the Martian mantle, *Geochimica et Cosmochimica Acta*, 64, 4083–4095.

- Budyko, M.I., 1969, The effect of solar radiation variations on the climate of the Earth, *Tellus*, 5, 611-619.
- Burton K.W., Gannoun A., Parkinson, J., 2010, Climate driven glacial–interglacial variations in the osmium isotope composition of seawater recorded by planktonic foraminifera. *Earth Planetary Science Letters*, 295, 258-268.
- Canfield, D.E., Poulton, S.W., and Narbonne, G.M., 2007, Late-Neoproterozoic deep-ocean oxygenation and the rise of animal life, *Science*, 315, 92–95.
- Canfield, D.E., Poulton, S.W., Knoll, A.H., Narbonne, G.M., Ross, G., Goldberg, T., and Strauss, H., 2008, Ferruginous conditions dominated later Neoproterozoic deep-water chemistry. *Science*, 321, 949–952.
- Clarke, M.J. and Farmer, N., 1976, Biostratigraphic nomenclature for Late Palaeozoic rocks in Tasmania, *Papers and Proceedings of the Royal Society of Tasmania*, 110, 91–109.
- Clayton, D.D., 1964, Cosmoradiogenic chronologies of nucleosynthesis, *Astrophys. J.*, 139, 637.
- Cohen, A.S., Coe, A.L., Bartlett J.M., and Hawkesworth, C.J., 1999, Precise Re–Os ages of organic-rich mudrocks and the Os isotope composition of Jurassic seawater, *Earth Planetary Science Letters*, 167, 159–173.
- Cohen, A. S. and Waters, F. G., 1996, Separation of osmium from geological materials by solvent extraction for analysis by thermal ionization mass spectrometry. *Anal. Chim.Acta*, 332, 269–275.
- Cohen, P.A., Schopf, J.W., Butterfield, N.J., Kudryavtsev, A., and Macdonald, F.A., 2011, Phosphate biomineralization in mid-Neoproterozoic protists. *Geology*, 39, 6, 539-542.
- Colodner, D.C., Boyle, E.A., and Edmond, J.M., 1993, The geochemical cycle of rhenium: a reconnaissance. *Earth and Planetary Science Letters*, 117, 205-221.
- Creaser, R.A., Sannigrahi, P., Chacko, T., and Selby, D., 2002, Further evaluation of the Re–Os geochronometer in organic-rich sedimentary rocks: A test of hydrocarbon maturation effects in the Exshaw Formation, Western Canada Sedimentary Basin. *Geochimica et Cosmochimica Acta*, 66, 3441-3452.

- Creaser, R.A. et al, 1991, Negative thermal ion mass spectrometry of osmium, rhenium, and iridium. *Geochimica et Cosmochimica Acta*, 55, 397-401.
- Creaser, R.A., 2012, *Re-Os Laboratory Visit*, personal communication.
- Crusius, J., Calvert, S., Pedersen, T., and Sage, D., 1996, Rhenium and molybdenum enrichments in sediments as indicators of oxic, suboxic, and sulfidic conditions of deposition, *Earth and Planetary Science Letters*, 145, 65-78.
- Dalia, K. and Ravizza, G., 2010, Investigation of an early Pleistocene marine osmium isotope record from the eastern equatorial Pacific, *Geochimica et Cosmochimica Acta*, 74, 4332-4345.
- Dickin, A.P., 2008, *Radiogenic Isotope Geology*. Cambridge University Press, Cambridge.
- Esser, B. K. and Turekian, K. K., 1993, The osmium isotopic composition of the continental crust. *Geochimica et Cosmochimica Acta*, 57, 3093-3104.
- Evans, D.A.D. and Raub, T.D., 2011, Neoproterozoic glacial palaeolatitudes: a global update. In: Arnaud, E., Halverson, G.P. & Shields-Zhou, G., eds., *The Geological Record of Neoproterozoic Glaciations*. Geological Society of London Memoirs, 36, 93-112.
- Eyles, N. & Januszczak, N., 2004, 'Zipper-rift': a tectonic model for Neoproterozoic glaciations during the breakup of Rodinia after 750 Ma. *Earth-Science Reviews*, 65, 1-73.
- Fielding, C.R., Frank, T.D., Isbell, J.L., Henry, L.C., and Domack, E.W., 2010, Stratigraphic signature of the late Paleozoic Ice Age in the Parmeener Supergroup of Tasmania, SE Australia, and inter-regional comparisons. *Papers in the Earth and Atmospheric Sciences*, Paper 263.
- Finlay, A. J., Selby, D., Osborne, M. J., 2011, Re-Os geochronology and fingerprinting of United Kingdom Atlantic margin oil: Temporal implications for regional petroleum systems. *Geology*, 39 (5) 475-478.
- Finlay, A. J., Selby, D., Osborne, M. J., 2012, Petroleum source rock identification of United Kingdom Atlantic margin oil fields and the western Canadian oil sands using platinum, palladium, osmium, and rhenium: Implications for global petroleum systems. *Earth and Planetary Science Letters*, 313-314, 95-104.

- Forsberg A. and Bjoroy M., 1983, A sedimentological and organic geochemical study of the Botneheia Formation, Svalbard, with special emphasis on the effects of weathering on the organic matter in shales. In: Bjorøy, M., Albrecht, P., Cornford, C. (eds) *Advances in Organic Geochemistry*, Wiley, 60–68.
- Frimmel, H.E., Klotzli, U., and Siegfried, P., 1996, New Pb-Pb single zircon age constraints on the timing of Neoproterozoic glaciation and continental break-up in Namibia. *The Journal of Geology*, 104, 459-508.
- Frimmel, H.E., Zartman, R.E., and Spath, A., 2001, Dating Neoproterozoic continental break-up in the Richtersveld Igneous Complex, South Africa, *The Journal of Geology*, 109, 493-508.
- Frimmel, H.E., 2011, The Kiagas and Numees Formations, Port Nolloth Group, in South Africa and Namibia. In: Arnaud, E., Halverson, G.P. & Shields-Zhou, G., eds., *The Geological Record of Neoproterozoic Glaciations*. Geological Society of London Memoirs, 36, 223-231.
- Frimmel, H.E., 2010, On the reliability of stable carbon isotopes for Neoproterozoic chemostratigraphic correlation. *Chemical Geology*, 182, 4, 239-253.
- Georgiev, S., Stein, H.J., Hannah, J.L., Wiess, H.M., Bingen, B., Xu, G., Rein, E., Hatlo, V., Loseth, H., Nali, M., and Piasecki, S., 2012, Chemical signals for oxidative weathering predict Re-Os isochronicity in black shales, East Greenland. *Chemical Geology*, 324-325, 108-121.
- Germis, G.J.B., 1972, New shelly fossils from Nama Group, South West Africa. *American Journal of Science*, 272, 752–761.
- Gramlich J. W., Murphy T. J., Garner E. L., and Shields W. R., 1973, Absolute isotopic abundance ratio and atomic weight of a reference sample of rhenium. *J. Res. National Bureau of Standards*, 77A, 691–697.
- Grotzinger, J., Watters, W., and Knoll, A., 2000, Calcified metazoans in thrombolite-stromatolite reefs of the terminal Proterozoic Nama Group, Namibia. *Paleobiology*, 26, 334–359.
- Halverson, G. P., Hoffman, P. F., Schrag, D. P., Maloof, A. C., Rice, A. H. N., 2005. Toward a Neoproterozoic composite carbon-isotope record. *Geological Society of America Bulletin* 117, 1181-1207.

- Halverson, G.P., 2006, A Neoproterozoic chronology. In: Xiao, S. and Kauffman, A.J. (eds) *Neoproterozoic Geobiology and Paleobiology*, Springer, 231-271.
- Halverson, G.P., Wade, B.P., Hurtgen, M.T., and Barovich, K.M., 2010, Neoproterozoic chemostratigraphy. *Precambrian Research*, 182, 4.
- Halverson, G.P. and Shields-Zhou, G., 2011, Chemostratigraphy and the Neoproterozoic glaciations. In: Arnaud, E., Halverson, G. P. & Shields-Zhou, G.A. (eds), *The Geological Record of Neoproterozoic Glaciations*. Geological Society of London, Memoir, 36, 51-66.
- Halverson, G.P., Maloof, A.C., Schrag, D.P., Dudas, F.O., and Hurtgen, M.T., 2007, Stratigraphy and geochemistry of a ca. 800 Ma negative carbon isotope interval in northeastern Svalbard. *Chemical Geology*, 237, 5-27.
- Harlan, S.S., Heaman, L.M., LeCheminant, A.N. and Premo, W.R., 2003, Gunbarrel mafic magmatic event: a key 780 Ma time marker for Rodinia plate reconstructions. *Geology*, 31, 1053-1056.
- Helz, G.R. and Dolor, M.K., 2012, What regulates rhenium deposition in euxinic basins? *Chemical Geology*, 304, 131-141.
- Henry, L.C., Isbell, J. L., Fielding, C. R., Domack, E. W., Frank, T. D., Fraiser, M. L., 2012, Proglacial deposition and deformation in the Pennsylvanian to Lower Permian Wynyard Formation, Tasmania: a process analysis. *Palaeogeography, Palaeoclimatology, Palaeoecology*, 315-316, 142-157.
- Herr, W., Hintenberger, H., and Voshage, H., 1954. Half-life of rhenium. *Physics Review*, 95, 1691.
- Hill, A.C., Arouri, K., Gorjan, P., and Walter, M.R., 2000, Geochemistry of marine and non-marine environments of a Neoproterozoic cratonic carbonate/evaporate: the Bitter Springs Formation, Central Australia. In: Grotzinger, J.P. and James, N.P. (eds) *Carbonate Sedimentation and Diagenesis in an Evolving Precambrian World*. SEPM Tulsa Special Publications, 67, 327-344.
- Hirt, B., Tilton, G. R., Herr, W., and Hoffmeister, W., 1963. The half-life of  $^{187}\text{Re}$ . In: Geiss, J. and Goldberg, E. Eds., *Earth Science and Meteoritics*. North Holland, Amsterdam.

- Hoffman, P. F., Kaufman, A. J., Halverson, G. P., Schrag, D. P., 1998, A Neoproterozoic snowball earth, *Science*, 281, 1342-1346.
- Hoffman, P.F. and Halverson, G.P., 2011, Neoproterozoic glacial record in the Mackenzie Mountains, northwest Canadian Cordillera. In: Arnaud, E., Halverson, G. P. & Shields-Zhou, G.A. (eds), *The Geological Record of Neoproterozoic Glaciations*, Geological Society of London, Memoir , 36, 397-411.
- Hosler, W.T., 1997, Geochemical events documented in inorganic carbon isotopes. *Palaeogeography, Palaeoclimatology, Palaeoecology*, 132, 173-182.
- Hyde, W. T., Crowley, T. J., Baum, S. K., Peltier, W. R., 2000, Neoproterozoic 'snowball Earth' simulations with a coupled climate/ice-sheet model, *Nature*, 405, 425-429.
- Jaffe, L. A., Peucker-Ehrenbrink, B., and Petsch, S. T., 2002, Mobility of rhenium, platinum group elements and organic carbon during black shale weathering. *Earth and Planetary Science Letters*, 198, 339-353.
- Jones, D.S., Maloof, A.C., Hurtgen, M.T., Rainbird, R.H., and Schrag, D.P., 2010, Regional and global chemostratigraphic correlation of the early Neoproterozoic Shaler Supergroup, Victoria Island, Northwestern Canada. *Precambrian Research*, 181, 43-63.
- Kasemann, S.A., Hawkesworth, C.J., Prave, A.R., Fallick, A.E., and Pearson, P.N., 2005, Boron and calcium isotope composition in Neoproterozoic carbonate rocks from Namibia: Evidence for extreme environmental change, *Earth and Planetary Science Letters*, 231, 1-2, 73-86.
- Kaufman, A.J., Knoll, A.H. and Narbonne, G.M., 1997, Isotopes, ice ages, and terminal Proterozoic earth history. *Proceedings of the National Academy of Sciences*, 94, 6600-6605.
- Kendall, B.S., Creaser, R.A., Ross, G.M., and Selby, D., 2004, Constraints on the timing of Marinoan 'Snowball Earth' glaciation by  $^{187}\text{Re}$ - $^{187}\text{Os}$  dating of a Neoproterozoic, post-glacial black shale in Western Canada. *Earth and Planetary Science Letters*, 222, 729-740.

- Kendall, B., Creaser, R. A., and Selby, D., 2009,  $^{187}\text{Re}$ - $^{187}\text{Os}$  geochronology of Precambrian organic-rich sedimentary rocks. *Geological Society, London, Special Publications* 326, 85-107.
- Kennedy, M., Mrofka, D., and von der Borch, C., 2008, Snowball Earth termination by destabilization of equatorial permafrost methane clathrate. *Nature*, 453, 642–645.
- Kirschvink, J. L., 1992 Late Proterozoic low-latitude global glaciation: the snowball Earth, *In: The Proterozoic Biosphere*, Schopf, J. W. and Klein, C. (eds.), Cambridge University Press, Cambridge, 51-52.
- Koide, M., Goldberg, E.D., Niemeyer, S., Gerlach, D., Hodge, V., Bertine, K.T., and Padova, A., 1991, Osmium in marine sediments. *Geochimica et Cosmochimica Acta*, 55, 1641-1648.
- Levasseur, S., Rachold, V., Birck, J., and Allegre, C.J., 2000, Osmium behavior in estuaries: the Lena River example. *Earth and Planetary Science Letters*, 177, 227-235.
- Lindner, M., Leich, D.A., Russ, G.P., Bazan J.M., and Borg, R.J., 1989, Direct determination of the half-life of  $^{187}\text{Re}$ . *Geochimica et Cosmochimica Acta*, 53, 1597–1606.
- Littke, R., Klusmann, U., Kroos, B., and Leythaeuser, D., 1991, Quantification of loss of calcite, pyrite, and organic matter due to weathering of Toarcian black shales and effects on kerogen and bitumen characteristics. *Geochimica et Cosmochimica Acta*, 55, 3369-3378.
- Ludwig, K.R., 2008. Isoplot/Ex, Version 4.15: A Geochronological Toolkit for Microsoft Excel. Geochronology Center, Berkeley.
- Luck, J.M., Birck J.L., and Allègre, C.J., 1980,  $^{187}\text{Re}$ - $^{187}\text{Os}$  systematics in meteorites: early chronology of the solar system and the age of the Galaxy, *Nature*, 283, 256–259.
- Martin, H., 1965, Beobachtungen zum Problem der jung-prakambrischen Glazialen Ablagerungen in Sudwestafrika. (Observations concerning the problem of the late Precambrian glacial deposits in South West Africa.) *Geologische Rundschau*, 54, 115– 127.

- Macdonald, F.A. and Roots, C.F., 2010. Upper Fifteenmile Group in the Ogilvie Mountains and correlations of early Neoproterozoic strata in the northern Cordillera. In: K.E. MacFarlane, L.H. Weston and L.R. Blackburn (eds.), *Yukon Exploration and Geology 2009*, Yukon Geological Survey, 237-252.
- Macdonald, F.A., Schmitz, J., Crowley, C., Roots, C., Jones, D., Maloof, A., Strauss, P., Cohen, D., Johnston, D., Schrag, D., 2010a, Calibrating the Cryogenian, *Science*, 327, 1241-1243.
- Macdonald, F.A., Cohen, P.A., Dudás, F.Ö., and Schrag, D.P., 2010b, Early Neoproterozoic scale microfossils in the Lower Tindir Group of Alaska and the Yukon Territory. *Geology*, 38, 143-146.
- Macdonald, F.A. and Cohen, P.A., 2011, The Tatonduk inlier, Alaska-Yukon border, In: *The Geological Record of Neoproterozoic Glaciations*, Arnaud, E., Halverson, G.P. and Shields-Zhou, G. (eds), Geological Society of London: London, 389-396.
- Maloof, A.C., Halverson, G.P., Kirschvink, J.L., Schrag, D.P., Weiss, B.P., and Hoffman, P.F., 2006, Combined paleomagnetic, isotopic, and stratigraphic evidence for true polar wander from the Neoproterozoic Akademikerbreen Group, Svalbard; *Geological Society of America Bulletin*, 118, 1099-1124.
- Morford, J.L., Martin, W.R., and Carney, C.M., 2012, Rhenium geochemical cycling: Insights from continental margins. *Chemical Geology*, 24, 73-86.
- Mustard, P.S. and Roots, C.F., 1997. Rift-related volcanism, sedimentation and tectonic setting of the Mount Harper Group, Ogilvie Mountains, Yukon Territory. Geological Survey of Canada, Bulletin 492.
- Naldrett, S. N. and Libby, W. F., 1948. Natural radioactivity of rhenium. *Physics Review* 73, 487-493
- Oxburgh, R., Pierson-Wickmann, A.C., Reisberg L., and Hemming, S., 2007, Climate-correlated variations in seawater  $^{187}\text{Os}/^{186}\text{Os}$  over the past 200,000 yr: evidence from the Cariaco basin, Venezuela. *Earth Planetary Science Letters*, 263, 246–258.
- Pegram, W.J., Krishnaswami, S., Ravizza G.E., and Turekian, K.K., 2002, The record of sea water  $^{187}\text{Os}/^{186}\text{Os}$  variation through the Cenozoic. *Earth Planet Science Letters*, 113, 569–576.

- Peucker-Ehrenbrink, B. and Hannigan, R. E., 2000, Effects of black shale weathering on the mobility of rhenium and platinum group elements. *Geology*, 28, 475-478.
- Peucker-Ehrenbrink, B. and Ravizza G., 2000, The marine osmium isotope record, *Terra Nova*, 12, 205–219.
- Peucker-Ehrenbrink, B. and Jahn, B.M., 2001, Rhenium-osmium isotope systematics and platinum group element concentrations: Loess and the upper continental crust. *Geochemistry, Geophysics, Geosystems*, 2, doi:10.1029/2001GC000172, only online.
- Peucker-Ehrenbrink, B. and Blum, J.D., 1998, Re–Os isotope systematics and weathering of Precambrian crustal rocks: implications for the marine Os isotope record. *Geochimica et Cosmochimica Acta*, 62, 3193–3203.
- Pierson-Wickmann, P.A., Reisberg, L., and France-Lanord, C., 2002, Behavior of Re and Os during low temperature alteration: Results from Himalayan soils and altered black shales. *Geochimica et Cosmochimica Acta*, 66, 9, 1539-1548.
- Porter, S.M., 2011, The rise of predators, *Geology*, 39, 6, 607-608.
- Porter S.M., Meisterfeld R., and Knoll A.H., 2003, Vase-shaped microfossils from the Neoproterozoic Chuar Group, Grand Canyon: A classification guided by modern testate amoebae: *Journal of Paleontology*, 77, 409–429.
- Porter S.M., Knoll A.H., 2000, Testate amoebae in the Neoproterozoic Era: Evidence from vase-shaped microfossils in the Chuar Group, Grand Canyon: *Paleobiology*, 26, 360–385.
- Ravizza, G. and Turekian, K.K., 1989, Application of the  $^{187}\text{Re}$ – $^{187}\text{Os}$  system to black shale geochronometry, *Geochimica et Cosmochimica Acta*, 53, 3257–3262.
- Ravizza, G., Turekian, K.K., and Hay, B.J., 1991, The geochemistry of rhenium and osmium in recent sediments from the Black Sea. *Geochimica et Cosmochimica Acta*, 55, 3741-3752.
- Rodgers, A.W., 1916, The geology of Namaqualand, *Transactions of the Geological Society of South Africa*, 18, 72-101.
- Rooney, A.D., Selby, D., Houzay, J-P., and Renne, P.R., 2010, Re-Os geochronology of Mesoproterozoic sediments from the Taoudeni basin, Mauritania: Implications for basin-wide correlations, supercontinent reconstruction and Re-Os

systematics of organic-rich sediments. *Earth and Planetary Science Letters*, 289, 486-496.

- Rooney, A.D., Chew, D.M., and Selby, D., 2011, Re–Os geochronology of the Neoproterozoic–Cambrian Dalradian Supergroup of Scotland and Ireland: Implications for Neoproterozoic stratigraphy, glaciations and Re–Os systematics. *Precambrian Research*, 182, 202-214.
- Rooney, A.D., 2011, Re–Os geochronology and geochemistry of Proterozoic sedimentary successions. *Doctoral Thesis*, Durham University.
- Rozefelds, A.C., Warren, A., Whitfield, A., and Bull, S., 2011, New evidence of large Permo-Triassic dicynodonts (Synapsida) from Australia, *Journal of Vertebrate Paleontology*, 31, 1158-1162.
- Russ, G. P. and Bazan, J. M., 1987, Osmium isotope ratio measurements by inductively coupled plasma source-mass spectrometry. *Analytical Chemistry* 59, 984-989.
- Schrag, D. P., Berner, R. A., Hoffman, P. F., Halverson, G. P., 2002, On the initiation of a snowball Earth, *Geochemistry, Geophysics, Geosystems*, 3, doi:10.1029/2001GC000219, only online.
- Selby, D., and Creaser, R.A., 2003, Re–Os geochronology of organic rich sediments: An evaluation of organic matter analysis methods. *Chemical Geology*, 200, 225-240.
- Selby, D., Creaser, R. A., Stein, H. J., Markey, R. J., and Hannah, J. L., 2007. Assessment of the <sup>187</sup>Re decay constant by cross calibration of Re–Os molybdenite and U–Pb zircon chronometers in magmatic ore systems. *Geochimica et Cosmochimica Acta* 71, 1999-2013.
- Selby, D. and Creaser, R. A., 2005. Direct radiometric dating of hydrocarbon deposits using rhenium-osmium isotopes. *Science*, 308, 1293-1295.
- Selby, D., Creaser, R. A., and Fowler, M. G., 2007, Re–Os elemental and isotopic systematics in crude oils. *Geochimica et Cosmochimica Acta*, 71, 378-386.
- Selby, D., 2011, Marine and lacustrine organic rich sedimentary unit time markers: Implications from rhenium and osmium geochronology. *American Geophysical Union Fall Meeting*, Abstract #V44A-04.

- Sharma M., Wasserburg, G.J., Hofmann, A.W., and Chakrapani, G.J., 1999, Himalayan uplift and osmium isotopes in oceans and rivers. *Geochimica et Cosmochimica Acta*, 63, 4005–4012.
- Shen, J. J., Papanastassiou, D. A., and Wasserburg, G. J., 1996. Precise Re-Os determinations and systematics of iron meteorites. *Geochimica et Cosmochimica Acta*, 60, 2887-2900.
- Shirely, S.B., and Walker, R.J., 1998, The Re-Os isotope system in cosmochemistry and high-temperature geochemistry, *Annu. Rev. Earth Planet. Sci.*, 26, 423–500.
- Singh, S.K., Trivedi J.R., and Krishnaswami, S., 1999, Re–Os isotope systematics in black shales from the Lesser Himalaya: their chronology and role in the  $^{187}\text{Os}/^{188}\text{Os}$  evolution of seawater, *Geochimica et Cosmochimica Acta*, 63, 2381–2392.
- Smoliar, M. I., Walker, R. J., and Morgan, J. W., 1996. Re-Os isotope constraints on the age of Group IIA, IIIA, IVA, and IVB iron meteorites. *Science*, 271, 1099-1102.
- Swanson-Hysell, N.L., Rose, C.V., Calmet, C., Halverson, G.P., Hurtgen, M.T., and Maloof, A.C., 2010, Cryogenian glaciation and onset of carbon-isotope decoupling. *Science*, 328, 608-611.
- Swanson-Hysell, N.L., Maloof, A.C., Evans, D.A.D., Kirschvink, J.L., Halverson, G.P. and Hurtgen, M.T., 2011, Constraints on Neoproterozoic paleogeography and Paleozoic orogenesis from paleomagnetic records of the Bitter Springs Formation, Amadeus Basin, central Australia, *American Journal of Science*.
- Tosca, N., Macdonald, F.A., Strauss, J.V., Johnston, D.T., Knoll, A.H., 2011, Sedimentary talc in Neoproterozoic carbonate successions, *Earth and Planetary Science Letters*, 306, 11-22.
- Turgeon, S.C. and Creaser, R.A., 2008, Cretaceous oceanic anoxic event 2 triggered by a massive magmatic episode. *Nature* 454, 323-326.
- Van Acken, D., Thomson, D., Rainbird, R.H., Creaser, R.A., 2012, Rhenium-Osmium dating of black shales from the Neoproterozoic Shaler Supergroup, Victoria Island, Canada. *Goldschmidt Conference 2012*, Session D #15.
- Vieira, L.C., Trindade, R.I.F., Nogueira, A.C.R., and Ader, M., 2007, Identification of a Sturtian cap carbonate in the Neoproterozoic Sete Lagoas carbonate platform, Bambuí Group, Brazil. *C. R. Geoscience*, 339, 240-258.

- Völkening J., Walczyk T., and Heumann K.G., 1991, Osmium isotope ratio determinations by negative thermal ionisation mass spectrometry. *International Journal of Mass Spectrometry and Ion Processes*, 105, 147–159.
- Walker, R. J. and Fassett, J. D., 1986. Isotope measurement of subnanogram quantities of rhenium and osmium by resonance ionization mass spectrometry. *Analytical Chemistry*, 58, 2923-2927.
- Woodhouse, O.B., Ravizza, G.E., Falkner, K.K., Statham, P.J., and Peucker-Ehrenbrink, B., 1999, Osmium in seawater: concentration and isotopic composition vertical profiles in the eastern Pacific Ocean. *Earth and Planetary Science Letters*, 173, 223-233.
- Yamashita, Y., Takahashi, Y., Haba, H., Enomoto, S., and Shimizu, H., 2007, Comparison of reductive accumulation of Re and Os in seawater-sediment systems. *Geochimica et Cosmochimica Acta*, 71, 3458-3475.
- Yang, G., Hannah, J. L., Zimmerman, A., Stein, H. J., and Bekker, A., 2009, Re-Os depositional age for Archean carbonaceous slates from the southwestern Superior Province: Challenges and insights. *Earth and Planetary Science Letters*, 280, 83-92.
- Young, G.M., 1988, Proterozoic plate tectonics, glaciation and iron-formations. *Sedimentary Geology*, 237, 107-126.
- Zheng, Y.F., Zhang, S.B., Zhao, Z.F., Wu, Y.B., Li, X., Li, Z., Wu, F.Y., 2007 Constraining zircon Hf and O isotopes in the two episodes of Neoproterozoic granitoids in South China: Implications for growth and reworking of continental crust. *Lithos*, 96, 127-150.
- Zhu, B., Becker, Jiang, S.Y., Pi, D.H., Fischer-Godde, M., and Yang, J.H., 2012, Re-Os geochronology of black shales from the Neoproterozoic Doushantuo Formation, Yangtze platform, South China. *Precambrian Research*, in press.